*Journal of Experimental Botany*, Vol. 67, No. 9 pp. 2699–2714, 2016
doi:10.1093/jxb/erw104 Advance Access publication 11 March 2016
This paper is available online free of all access charges (see http://jxb.oxfordjournals.org/open_access.html for further details)

RESEARCH PAPER

# Temperature response of bundle-sheath conductance in maize leaves

**Xinyou Yin*, Peter E.L. van der Putten, Steven M. Driever and Paul C. Struik**

Centre for Crop Systems Analysis, Department of Plant Sciences, Wageningen University, PO Box 430, 6700 AK Wageningen, The Netherlands

*Correspondence: Xinyou.Yin@wur.nl

Received 20 December 2015; Accepted 16 February 2016

Editor: Susanne von Caemmerer, Australian National University

## Abstract

**A small bundle-sheath conductance ($g_{bs}$) is essential for the $C_4$ $CO_2$-concentrating mechanism to suppress photorespiration effectively. To predict the productivity of $C_4$ crops accurately under global warming, it is necessary to examine whether and how $g_{bs}$ responds to temperature. We investigated the temperature response of $g_{bs}$ in maize by fitting a $C_4$ photosynthesis model to combined gas exchange and chlorophyll fluorescence measurements of irradiance and $CO_2$ response curves at 21% and 2% $O_2$ within the range of 13.5–39 °C. The analysis was based on reported kinetic constants of $C_4$ Rubisco and phospho*enol*pyruvate carboxylase and temperature responses of $C_3$ mesophyll conductance ($g_m$). The estimates of $g_{bs}$ varied greatly with leaf temperature. The temperature response of $g_{bs}$ was well described by the peaked Arrhenius equation, with the optimum temperature being ~34 °C. The assumed temperature responses of $g_m$ had only a slight impact on the temperature response of $g_{bs}$. In contrast, using extreme values of some enzyme kinetic constants changed the shape of the response, from the peaked optimum response to the non-peaked Arrhenius pattern. Further studies are needed to confirm such an Arrhenius response pattern from independent measurement techniques and to assess whether it is common across $C_4$ species.**

**Key words:** Diffusive resistance, maximum PEPc activity, maximum Rubisco activity, modelling, warming effect, *Zea mays*.

## Introduction

$C_4$ crop species have the $CO_2$-concentrating mechanism (CCM) in photosynthesis, which raises the partial pressure of $CO_2$ in bundle-sheath cells to a very high level, thereby minimizing the oxygenation activity of Rubisco and the loss by photorespiration (Hatch *et al.*, 1995). This explains why $C_4$ food crops such as maize (*Zea mays* L.) generally have higher productivities than their $C_3$ counterparts (Ort and Long, 2014), at least under relatively warm conditions, and why $C_4$ species are preferred as a major source of sustainable bioenergy production (Heaton *et al.*, 2008; Slattery and Ort, 2015).

The CCM mechanism in $C_4$ crops requires a number of biochemical, physical, and structural adaptations, especially the Kranz anatomy including the specialization of the mesophyll and bundle-sheath cells (Hatch *et al.*, 1995; Leegood, 2002; Kromdijk *et al.*, 2014). In $C_4$ photosynthesis, $CO_2$ is first fixed via phospho*enol*pyruvate carboxylase (PEPc) in mesophyll cells into $C_4$ acids, which are then transported into bundle-sheath cells where the $C_4$ acids are decarboxylated and the released $CO_2$ is refixed by Rubisco. An efficient CCM would require that (i) PEPc has higher $CO_2$ affinity and carboxylation capacity than Rubisco; and (ii) the rate of $CO_2$ leakage from bundle-sheath cells back into mesophyll cells ($L$) is low.

This $CO_2$ leakage rate $L$ depends on both the bundle-sheath conductance for $CO_2$ ($g_{bs}$) and the gradient between the $CO_2$ concentration in mesophyll cells ($C_m$) and that around the carboxylation sites in bundle-sheath cells ($C_c$): $L=g_{bs}(C_c-C_m)$

(von Caemmerer and Furbankm 1999; Kromdijk *et al.*, 2014). Therefore, $g_{bs}$ is an important parameter for the effectiveness of CCM. We have previously analysed how $g_{bs}$ responds to nitrogen supply, and showed that $g_{bs}$ increases with increasing leaf nitrogen content (Yin *et al.*, 2011)—a trend similar to that found for mesophyll conductance ($g_m$) in response to leaf photosynthetic capacity in $C_3$ photosynthesis (e.g. Loreto *et al.*, 1992). It has been well established that $g_m$ in $C_3$ photosynthesis responds to leaf temperature (Bernacchi *et al.*, 2002; Warren and Dreyer, 2006; Yamori *et al.*, 2006; Scafaro *et al.*, 2011; Evans and von Caemmerer, 2013; Walker *et al.*, 2013), although the effects differ greatly among species (von Caemmerer and Evans, 2015). Massad *et al.* (2007) have parameterized temperature dependence of some $C_4$ parameters such as the maximum rates of PEPc carboxylation ($V_{pmax}$), of Rubisco carboxylation ($V_{cmax}$), and of electron transport. However, there is hardly any information in the literature on whether and how $g_{bs}$ responds to leaf temperature. Reports of Kubien *et al.* (2003) and von Caemmerer *et al.* (2014) on the temperature effect on leakiness (ϕ; which is defined as $L/V_p$, where $V_p$ is the PEPc carboxylation rate) indirectly suggest that $g_{bs}$, among many $C_4$ parameters, may (co-)vary with temperature. To the best of our knowledge, only one study (Kiirats *et al.*, 2002) has directly reported on the temperature response of $g_{bs}$: $g_{bs}$ increased almost linearly with increasing leaf temperature within the range of 16–35 °C. That study used a PEPc mutant of *Amaranthus edulis* with a defective $C_4$ cycle. However, concerns have been raised about potential alterations of Rubisco kinetic constants, gas diffusion resistance, and bundle-sheath cell structure by the PEPc mutation (He and Edwards, 1996).

Given the effect of elevating atmospheric $CO_2$ and global warming, it is necessary to assess the production potential of $C_4$ species, as well as whether their relative advantages over $C_3$ species vary, under climate change. Like the widely used $C_3$ photosynthesis model of Farquhar *et al.* (1980), the $C_4$ biochemical models (Berry and Farquhar, 1978; von Caemmerer and Furbank, 1999) or their variants (Collatz *et al.*, 1992; Chen *et al.*, 1994; Yin and Struik, 2009*a*) are now increasingly coupled with stomatal conductance models and applied to a general ecosystem or crop simulation framework. However, these modelling studies all assume that $g_{bs}$ does not vary with temperature, even when applied to a wide range of natural field environments. To apply the biochemical $C_4$ photosynthesis model to assess the (relative) production potentials and their response to climate change variables, information on the effects of temperature on $g_{bs}$ is urgently needed. The objectives of this study are to assess whether or not $g_{bs}$ in leaves of a maize cultivar responds to leaf temperature and, if so, to quantify the magnitude of this effect over a wide range of temperatures. To that end, we use the method of Yin *et al.* (2011) that can estimate $g_{bs}$ by fitting a $C_4$ photosynthesis model to a wide range of data covering different amounts of photorespiration.

## Materials and methods

### *Experimental set-up*

An experiment was conducted in a glasshouse at Wageningen University, using maize cv. 'Atrium'. To spread out the measurement work in time, a weekly staggered sowing was carried out on 28 August and 4, 10, and 18 September 2014, respectively, to grow plants for four replicate measurements. Plants were transplanted 7 d after sowing to pots of 12 litres, with one plant per pot. The initial soil nutrient contents were: 1.23 g of nitrogen, 0.69 g of phosphate, and 2.49 g of potassium per pot. Extra nutrients came from 10.3 g per pot of a slow-release fertilizer 'Osmocote Pro' (which contained 17% N, 11% $P_2O_5$, 10% $K_2O$, 2% MgO plus trace elements). Temperature in the glasshouse was 27 ± 2 °C for daytime and 21 ± 1 °C for night-time . Photoperiod was maintained at 12 h $d^{-1}$ (8:00–20:00 h), and relative humidity ranged between 60% and 70%. Of the photosynthetically active radiation incident on the glasshouse, 60% was transmitted to plant level. During daytime, supplemental light from 600 W HPS Hortilux Schréder lamps (Monster, The Netherlands; 0.4 lamps $m^{-2}$) was switched on automatically as soon as the global solar radiation incident on the glasshouse dropped below 400 W $m^{-2}$, and then switched off if it exceeded 500 W $m^{-2}$. The supplementary light largely ensured that, despite the staggered sowing, plants for measurements grew under similar light intensities.

### *Photosynthesis measurements*

After growth in the glasshouse for ~6 weeks, plants were moved to a climate room illuminated by cool-white fluorescent tubes (~350 µmol $m^{-2}$ $s^{-1}$ at leaf level), where all measurements were undertaken. We used an LI-6400XT open gas exchange system with an integrated fluorescence chamber head, enclosing 2 $cm^2$ areas, for combined gas exchange and chlorophyll fluorescence measurements, which were done on fully expanded leaves at the seventh leaf layer counted from below. The $CO_2$ response curves were taken under both 21% and 2% $O_2$ conditions, and the ambient $CO_2$ ($C_a$) steps were: 370, 200, 100, 85, 70, 55, 370, 370, 370, 500, 700, and 1500 µmol $mol^{-1}$ (~4 min per step) while keeping incident irradiance ($I_{inc}$) at 1500 µmol $m^{-2}$ $s^{-1}$ (while measurements were done four times at 370 µmol $mol^{-1}$, data of only the first and fourth times were included for the analysis). For light response curves, $I_{inc}$ was of the order of 2000, 1500, 1000, 500, 200, 100, 80, 60, 40, and 20 µmol $m^{-2}$ $s^{-1}$ (~8 min per step), while keeping $C_a$ either at 250 µmol $mol^{-1}$ for 21% $O_2$ or at 1000 µmol $mol^{-1}$ for 2% $O_2$ conditions; this was done to induce different levels of photorespiration. Gas from a cylinder containing a mixture of $N_2$ and required $O_2$ was humidified and supplied via an overflow tube to the air inlet of the LI-6400XT where $CO_2$ was blended with the gas, and the IRGA calibration was adjusted for $O_2$ composition of the gas mixture according to the manufacturer's instructions.

Each curve was made at six set-point leaf temperatures (13.5, 18, 25, 30, 34, and 39 °C), of which extreme temperatures (13.5, 34, and 39 °C) were achieved not only by setting the temperature in the LI-6400XT measuring head but also by adjusting the temperature of the climate room. Measurement of one replicate took 5 d and was done on the same leaf for all temperatures. Any influence of different measuring days was minimized by randomizing temperatures and measuring days among the replicates. In total, 48 (i.e. 6 temperatures×4 replicates×2 $O_2$ levels) light response curves and 48 $CO_2$ response curves were generated. Leaf-to-air vapour pressure difference increased with leaf temperature, but was always within the range of 0.5–2.0 kPa, within which little impact of vapour pressure difference on stomatal conductance is expected (Bernacchi *et al.*, 2002). The measurement flow rate was 400 µmol $s^{-1}$. $CO_2$ exchange rates were corrected for $CO_2$ leakage into and out of the leaf cuvette, based on measurements at specific temperatures using the same flow rate on boiled leaves across a range of $CO_2$ levels, and intercellular $CO_2$ levels ($C_i$) were then re-calculated.

For each step of light or $CO_2$ response, when the $CO_2$ exchange rate reached steady state, steady-state fluorescence ($F_s$) was measured. Dwyer *et al.* (2007) have shown that for $C_4$ leaves, the multiple-flash method is more reliable than the traditional single-flash method in measuring the maximum fluorescence ($F_m'$). The $F_m'$ was therefore obtained from using the multiphase flashes: the flash intensity was ~8000 µmol $m^{-2}$ $s^{-1}$ during phase 1 for a duration of 300 ms, was attenuated by 35% during phase 2 for ~300 ms, and was back to

~8000 µmol $m^{-2}$ $s^{-1}$ for phase 3 of 300 ms. The intercept of the linear regression of fluorescence yields against the inverse of the flash intensity during phase 2 gives the estimate of $F_m'$ (Loriaux *et al.* 2013). The apparent operating efficiency of photosystem II (PSII) $e^-$ transport was obtained as: $\Delta F/F_m' = (F_m' - F_s)/F_m'$ (Genty *et al.*, 1989; Schreiber *et al.*, 1995).

The portions of the leaf used for above measurements were excised afterwards, with a punch that produced a disc of ~5 $cm^2$ per leaf portion. The leaf discs were then weighed after drying at 70 °C to constant weight, and total N content was analysed using an element C/N analyser (Flash 2000, Thermo Scientific) based on the Micro-Dumas combustion method.

### *Modelling*

The model of von Caemmerer and Furbank (1999), as modified by Yin *et al.* (2011), was used to estimate $g_{bs}$ (see Supplementary appendix A at *JXB* online). The first modification was to include all four combinations of rate limitations to describe $CO_2$ and light response curves of the $C_4$ leaf $CO_2$ assimilation rate ($A$) more smoothly:

$$A = \min\left(A_{EE}, A_{ET}, A_{TE}, A_{TT}\right) \quad (1)$$

where $A_{EE}$ is the net $CO_2$ assimilation rate when both $C_4$ and $C_3$ cycles are limited by enzyme activity, $A_{ET}$ is the net rate when the $C_4$ cycle is limited by enzyme activity and the $C_3$ cycle is limited by $e^-$ transport, $A_{TE}$ is the rate when the $C_4$ cycle is limited by $e^-$ transport and the $C_3$ cycle is limited by enzyme activity, and $A_{TT}$ is the rate when both $C_4$ and $C_3$ cycles are limited by $e^-$ transport. The formulation of von Caemmerer and Furbank (1999) used only two combinations, namely $A=\min(A_{EE},A_{TT})$. The second modification was to consider mesophyll conductance ($g_m$) explicitly so that $A$ is modelled using $C_i$ (rather than mesophyll $CO_2$ level $C_m$) as input, as $C_m$ is not measured. The model considering $g_m$ becomes more complicated, and Yin *et al.* (2011) presented an analytical solution for each of the four limitations (see Supplementary appendix A). The third modification was to use the potential rate of ATP production ($J_{atp}$), instead of the potential rate of $e^-$ transport rate ($J$), because energy is partitioned between $C_4$ and $C_3$ cycles ultimately in terms of ATP (rather than in terms of electron) requirement. von Caemmerer and Furbank (1999) implicitly assumed that $J_{atp}=J$, whereas the analysis of Yin and Struik (2012) showed that $J_{atp}$ may not equal $J$.

We estimated the value of $J_{atp}$ empirically from chlorophyll fluorescence measurements, according to Yin *et al.* (2011):

$$J_{atp} = s' I_{inc} (\Delta F / F_m') / (1 - x) \quad (2)$$

where $x$ is the fraction of ATP partitioned to the $C_4$ cycle (set to 0.4; von Caemmerer and Furbank 1999), and $s'$ is a lumped parameter resulting as the slope from the linear regression of $A$ measured under low irradiances (≤500 µmol $m^{-2}$ $s^{-1}$) against $I_{inc}(\Delta F/F_m')/3$ using only the data at 2% $O_2$ combined with high $CO_2$, at which photorespiration is suppressed. The intercept of the same linear regression will give the estimate of day respiration ($R_d$) (Yin *et al.*, 2011). It is worth noting the importance of only using an $e^-$ transport-limited range of data for estimating $s'$ which calibrates for the impact of any basal alternative $e^-$ transport. Impacts of any additional alternative $e^-$ transport, such as under high $I_{inc}$ or low $C_i$ conditions, arising from the higher $J_{atp}$ than required for $C_4$ and $C_3$ cycles, are accounted for by Equation 1 via assigning to enzyme activity-limited rates.

The model of von Caemmerer and Furbank (1999) was proposed for the reference temperature 25 °C. To be applied for a range of varying temperatures, the potential variation of relative $O_2/CO_2$ diffusivities and solubilities with temperature needs to be quantified. This is presented in Supplementary appendix B, based on data in the literature (e.g. Frank *et al.*, 1996; Han and Bartels, 1996).

### *Pre-determination of some photosynthetic parameters*

To use the model to estimate $g_{bs}$, a number of other input parameter values are required (see Table 1 for parameter definitions). The Rubisco kinetic parameters ($V_{cmax}$, γ*, $K_{mC}$, and $K_{mO}$), the PEPc Michaelis–Menten constant ($K_p$), and $R_d$ are expected to increase with temperature, and this is conventionally described by an Arrhenius function normalized at 25 °C:

$$\text{Parameter} = \text{Parameter}_{25} \cdot e^{\frac{E}{R}\left(\frac{1}{298} - \frac{1}{273+T}\right)} \quad (3)$$

where $R$ is the universal gas constant (0.008314 kJ $K^{-1}$ $mol^{-1}$) and $E$ is the activation energy (kJ $mol^{-1}$) for the parameter. It is impossible to derive a complete set of *in vivo* kinetic constants of $C_4$ photosynthesis, and we mostly used *in vitro* values as reported in the literature. Values of γ*, $K_{mC}$, $K_{mO}$, and $K_p$ at the reference temperature 25 °C (Table 1) were the same as those we used previously (Yin *et al.*, 2011), based on data for maize (e.g. Cousins *et al.*, 2010). Other parameter values are hardly available for maize, and the values used are summarized below.

(i) Sage (2002), Kubien *et al.* (2003), and Perdomo *et al.* (2015) reported the activation energy $E$ of $V_{cmax}$. Sage's data on $E_{Vcmax}$ for seven $C_4$ species range from 50.1 kJ $mol^{-1}$ for *Cynodon dactylon* and 53.5 kJ $mol^{-1}$ for *Flaveria trinervia* to 68.0 kJ $mol^{-1}$ for *Amaranthus retroflexus*. Kubien *et al.* (2013) reported 56.1 kJ $mol^{-1}$ within 18–42 °C for *Flaveria bidentis*. $E_{Vcmax}$ values reported by Perdomo *et al.* (2015) for *Flaveria bidentis* and *Flaveria trinervia* were 47.6 kJ $mol^{-1}$ and 48.8 kJ $mol^{-1}$, respectively. Despite the variation of $E_{Vcmax}$ even for the same species, $E_{Vcmax}$ for $C_4$ species did not differ greatly from that for $C_3$ species (Sage, 2002; Perdomo *et al.*, 2015). The average $E_{Vcmax}$ of the three reports for $C_4$ species was used here (Table 1).

(ii) Jordan and Ogren (1984) were the first to report on Rubisco specificity from 5 °C to 35 °C of a $C_4$ species *Amaranthus hybridus*, from which we derived the activation energy for γ* (Table 1). This estimate is quite similar to the value of Bernacchi *et al.* (2002) for $C_3$ species, and the report of Boyd *et al.* (2015) for a $C_4$ species *Setaria viridis*.

(iii) The activation energy for $K_{mC}$ of $C_4$ Rubisco was based on the recent report of Perdomo *et al.* (2015) on two *Flaveria* $C_4$ species (Table 1).

(iv) Little is known for the activation energy for $K_{mO}$ of $C_4$ Rubisco, and Table 1 gives its value that we derived from data of Perdomo *et al.* (2015) on activation energies for specificity ($S_{c/o}$) and $K_{mC}$, using the formula $K_{mO}=S_{c/o}K_{mC}(V_{omax}/V_{cmax})$ (where $V_{omax}$ is the maximum oxygenation rate of Rubisco) and assuming that the $V_{omax}$:$V_{cmax}$ ratio does not vary with temperature (i.e. activation energy for this ratio=0). The latter assumption was based on reports that the activation energy for $V_{omax}$:$V_{cmax}$ of $C_3$ Rubisco is either small (Bernacchi *et al.*, 2001) or inconsistent (either positive or negative) across species (von Caemmerer and Quick, 2000; Walker *et al.*, 2013). This is in line with the $C_3$ photosynthesis modelling (Farquhar *et al.*, 1980) that $V_{omax}$:$V_{cmax}$ is set to be independent of temperature. The derived activation energy for $K_{mO}$ (15.1 kJ $mol^{-1}$) is only slightly higher than 10.5 (±4.8) kJ $mol^{-1}$, the value that Boyd *et al.* (2015) published for *S. viridis* while we were revising our paper. Our $E_{KmO}$ corresponds to a $Q_{10}$ factor of ~1.23, very close to the value 1.20 that Chen *et al.* (1994) used. Sensitivity analysis showed that the temperature response of $g_{bs}$ was least sensitive to $E_{KmO}$ (see the Results).

**Table 1.** *Model input parameters, with their default values as derived from the literature or in this study*

| Symbol | Definition | Value | Source |
|---|---|---|---|
| $\alpha$ | Fraction of PSII activity in the bundle sheath | 0.1 | Chapman *et al.* (1980) |
| $R_m$ | Mitochondrial respiration in the mesophyll | $0.5R_d$ | von Caemmerer and Furbank (1999) |
| $x$ | Fraction of ATP allocated to the $C_4$ cycle | 0.4 | von Caemmerer and Furbank (1999) |
| $K_{p25}$ | Michaelis–Menten constant of PEPc for $CO_2$ at 25 °C | 40 μbar | Leegood and von Caemmerer (1989); Pfeffer and Peisker (1995) |
| $K_{mC25}$ | Michaelis–Menten constant of Rubisco for $CO_2$ at 25 °C | 485 μbar | Cousins *et al.* (2010) |
| $K_{mO25}$ | Michaelis–Menten constant of Rubisco for $O_2$ at 25 °C | 146 000 μbar | Cousins *et al.* (2010) |
| $\gamma^*_{25}$ | Half the reciprocal of Rubisco specificity at 25 °C | 0.0001747 | Cousins *et al.* (2010) |
| $E_{Vcmax}$ | Activation energy for $V_{cmax}$ (maximum Rubisco activity) | 53.4 kJ mol$^{-1}$ | Sage (2002); Kubien *et al.* (2003); Perdomo *et al.* (2015) |
| $E_{\gamma^*}$ | Activation energy for $\gamma^*$ | 27.4 kJ mol$^{-1}$ | Derived from data of Jordan and Ogren (1984) |
| $E_{KmC}$ | Activation energy for $K_{mC}$ | 35.6 kJ mol$^{-1}$ | Perdomo *et al.* (2015) |
| $E_{KmO}$ | Activation energy for $K_{mO}$ | 15.1 kJ mol$^{-1}$ | Derived from results of Perdomo *et al.* (2015) |
| $E_{Vpmax}$ | Activation energy for $V_{pmax}$ (maximum PEPc activity) | 37.0 kJ mol$^{-1}$ | Derived from data of Chinthapalli *et al.* (2003) |
| $D_{Vpmax}$ | Deactivation energy for $V_{pmax}$ | 214.5 kJ mol$^{-1}$ | Derived from data of Chinthapalli *et al.* (2003) |
| $S_{Vpmax}$ | Entropy term for $V_{pmax}$ | 0.663 kJ K$^{-1}$ mol$^{-1}$ | Derived from data of Chinthapalli *et al.* (2003) |
| $E_{Kp}$ | Activation energy for $K_p$ | 68.1 kJ mol$^{-1}$ | Estimated in our report (see text) |
| $E_{gm}$ | Activation energy for $g_m$ (mesophyll conductance) | 49.6 kJ mol$^{-1}$ | Bernacchi *et al.* (2002) |
| $D_{gm}$ | Deactivation energy for $g_m$ | 437.4 kJ mol$^{-1}$ | Bernacchi *et al.* (2002) |
| $S_{gm}$ | Entropy term for $g_m$ | 1.4 kJ K$^{-1}$ mol$^{-1}$ | Bernacchi *et al.* (2002) |

PEPc, phospho*enol*pyruvate carboxylase; PSII, photosystem II.

(v) $V_{pmax}$ follows an optimum response to temperature (Chinthapalli *et al.*, 2003; Massad *et al.*, 2007; Boyd *et al.*, 2015). This optimum response can be described by the peaked Arrhenius function (Medlyn *et al.* 2002):

$$\text{Parameter} = \text{Parameter}_{25} e^{\frac{E}{R}\left(\frac{1}{298}-\frac{1}{273+T}\right)} \frac{1+e^{(S-D/298)/R}}{1+e^{[S-D/(273+T)]/R}} \quad (4)$$

where $S$ is an entropy term (kJ K$^{-1}$ mol$^{-1}$), and $E$ and $D$ are energies of activation and deactivation (kJ mol$^{-1}$), respectively. Differentiating Equation 4 gives the optimum temperature $T_{opt}$ (°C) as:

$$T_{opt} = \frac{D}{S + R\ln(D/E - 1)} - 273 \quad (5)$$

We used the *in vitro* data of Chinthapalli *et al.* (2003) for *Amaranthus hypochondriacus*, which cover a very wide range of temperatures from 15 °C to 50 °C, to fit Equation 4 to derive values for $S$, $E$, and $D$ of $V_{pmax}$ (Table 1). These estimates resulted in an estimate of $T_{opt}$=44.4 °C.

(vi) Little is known about the activation energy of $K_p$. We examined the initial slope of $A$–$C_i$ curves at 2% $O_2$, since $A$ at low $C_i$ is limited by the PEPc activity (Sage and Kubien, 2007) and can be approximated to $C_iV_{pmax}/(C_i+K_p)-R_m$ (von Caemmerer and Furbank, 1999). The first-order derivative of this equation, $dA/dC_i$, is $K_pV_{pmax}/(C_i+K_p)^2$, and was set to equal the slope value of the initial linear part of the $A$–$C_i$ curve. The initial linear slope of the $A$–$C_i$ curve followed an optimum response to temperature (see the Results) and this response is expected to result from temperature responses of both $K_p$ and $V_{pmax}$. Using the pre-estimated temperature response parameters of $V_{pmax}$, we then derived the activation energy for $K_p$ by fitting combined Equation 3 and $dA/dC_i=K_pV_{pmax}/(C_i+K_p)^2$ to data on the initial linear slope of the $A$–$C_i$ curves over the six temperatures. We will confirm our estimate on $E_{Kp}$ from fitting a full model to data of the initial part of $A$–$C_i$ curves (see the Results).

(vii) Mesophyll conductance ($g_m$) may be a significant limiting factor for $C_4$ photosynthesis (Pfeffer and Peisker, 1998), has an impact on estimation of leakiness (von Caemmerer *et al.*, 2014), and its role in estimating $g_{bs}$ has yet to be quantified. However, $g_m$ for $C_4$ photosynthesis is hard to estimate (Pfeffer and Peisker, 1998; Barbour *et al.*, 2016), let alone its temperature response parameters. We took the widely used values of Bernacchi *et al.* (2002) for $g_m$ in $C_3$ photosynthesis, which include $E$, $D$, and $S$ as quantified in Equation 4 (Table 1). This approach assumes that $C_3$ and $C_4$ photosynthesis have a similar relative response of $g_m$ to temperature, although $g_m$ in $C_4$ does not involve chloroplast-related resistance components. Our assumption for the same relative response of the overall $g_m$ to temperature for $C_3$ and $C_4$ leaves will be tested through a sensitivity analysis.

### *Curve fitting and sensitivity analysis*

With all these parameters pre-determined, we estimated $g_{bs}$ of the six temperatures as well as $g_{m25}$, $V_{cmax25}$, $V_{pmax25}$ (i.e. $g_m$, $V_{cmax}$, $V_{pmax}$ at 25 °C, respectively), by the non-linear curve-fitting using Equation 1 in combination with solutions in Supplementary appendix A. We used a dummy variable approach (Yin *et al.*, 2009), in which we introduced six dummy variables to correspond to six temperatures, allowing us to estimate treatment-specific parameters (i.e.

$g_{bs}$ at six temperatures) and common parameters (i.e. $g_{m25}$, $V_{cmax25}$, and $V_{pmax25}$) simultaneously. The statistical fitting algorithms, implemented in SAS, autoassigned the range of data points to each of the four limitations as defined by Equation 1. The $g_{bs}$ estimates when plotted against leaf temperature followed an optimum response (see the Results), and parameters characterizing this response were derived from fitting the estimated $g_{bs}$ to Equation 4. All required curve fitting was carried out using the least-squares non-linear regression with the GAUSS method in PROC NLIN of SAS (SAS Institute Inc., Cary, NC, USA). The SAS codes for estimating $g_{bs}$ parameters are available from the corresponding author upon request.

Regardless of the technique used, estimates for kinetic constants of Rubisco are full of uncertainties (Kubien *et al.*, 2008; Cousins *et al.*, 2010), so are the constants of PEPc (Pfeffer and Peisker, 1998) and of $g_m$ (Silim *et al.*, 2010; Walker *et al.*, 2013). Also, the input values of some constants were not determined exclusively for maize. Therefore, a full sensitivity analysis on the $g_{bs}$ estimates was conducted with respect to these input parameters in Table 1, except for $x$ and α. The value of $x$ is expected to be very invariant in terms of the ATP requirement between $C_4$ and $C_3$ cycles (von Caemmerer and Furbank, 1999), and a previous analysis (Yin *et al.*, 2011) showed little sensitivity of $g_{bs}$ to parameter α.

## Results

### *Overall response curves of A and ΔF/F$_m$′ to CO$_2$ and irradiance*

Our experimental results at the six temperatures showing typical irradiance and $CO_2$ responses of the $C_4$ photosynthesis rate were obtained (Fig. 1). The non-photorespiratory condition (2% $O_2$ combined with 1000 µmol mol$^{-1}$ $C_a$) had a moderate positive effect on the irradiance response curves, compared with the curves of 21% $O_2$ combined with 250 µmol mol$^{-1}$ $C_a$. Temperature strongly affected both irradiance and $CO_2$ response curves, and its effect was more significant from 13.5 °C to 25 °C than from 25 °C to 39 °C. The maximum photosynthesis was observed at ~34 °C. The effect of temperature on photosynthesis was reflected by the data for temperature effect on $\Delta F/F_m'$, the apparent operating efficiency of PSII $e^-$ transport (Fig. 2).

### *Estimates of s′ and R$_d$*

The relationship between $A$ and $I_{inc}(\Delta F/F_m')/3$ measured at low irradiances (≤500 µmol m$^{-2}$ s$^{-1}$) under non-photorespiratory conditions was linear for all temperatures (Fig. 3). The slope of this linear relationship gives the estimate for $s'$, a lumped parameter for calculating $J_{atp}$ (see Equation 2), and its intercept gives the estimate of $R_d$ (day respiration). Data points of higher irradiances (>500 µmol m$^{-2}$ s$^{-1}$) lay below the linear trend for all temperatures (Fig. 3), indicating that $A$ was limited by $A_{EE}$ or $A_{TE}$ (see Equation 1) at high irradiances.

The estimated calibration factor $s'$ varied from 0.25 to 0.34, and its response to temperature can be empirically described by a quadratic equation with the optimum temperature at ~30 °C (Fig. 4a). As expected, the estimated values of $R_d$ increased with increasing temperature (Fig. 4b). This response was well described by the Arrhenius equation, Equation 3, with the estimated $R_d$ at 25 °C being 1.95 µmol m$^{-2}$ s$^{-1}$ and the activation energy being 41.9 kJ mol$^{-1}$ (Table 2).

### *Initial slope of A–C$_i$ curves*

The $A$–$C_i$ curves at 2% $O_2$ for the first three (for 13.5 °C) or four (for the remaining temperatures) points were essentially linear (Supplementary Fig. S1). The slope of this initial linear section of $A$–$C_i$ curves at six temperatures followed an optimum response to temperature (Fig. 5), and this response is expected to result from temperature responses of both $K_p$ and $V_{pmax}$. Using the pre-estimated temperature response parameter values of $V_{pmax}$ (Table 1), we estimated the activation energy for $K_p$ by fitting combined Equation 3 and $dA/dC_i = K_p V_{pmax}/(C_i+K_p)^2$ to data in Fig. 5 for the initial slope of $A$–$C_i$ curves at the six temperatures. The estimated $E_{Kp}$, the activation energy for $K_p$, was 68.1 (SE 6.8) kJ mol$^{-1}$ (Table 1).

### *Estimated response of g$_{bs}$ to temperature*

With $s'$, $R_d$, and $E_{Kp}$ pre-fixed as presented above and other input parameters available (Table 1), we were able to estimate $g_{m25}$, $V_{cmax25}$, $V_{pmax25}$, and $g_{bs}$ of the six temperatures by fitting our model (Equation 1 combined with solutions given in the Supplementary data) to all data collected in the experiment. The model described the whole data set across $A$–$C_i$ and $A$–$I_{inc}$ curves at 2% and 21% $O_2$, with $R^2$=0.98 and relative root-mean-square error rRMSE (RMSE×100/the mean of measured $A$)=12.0%, and a plot comparing modelled and measured $A$–$I_{inc}$ and $A$–$C_i$ curves is given in Supplementary Fig. S2 for 21% $O_2$. The obtained $g_{m25}$ was 1.33 mol m$^{-2}$ s$^{-1}$, $V_{cmax25}$ was 49.0 µmol m$^{-2}$ s$^{-1}$, and $V_{pmax25}$ was 119.2 µmol m$^{-2}$ s$^{-1}$ (Table 2), meaning that the $V_{pmax25}$:$V_{cmax25}$ ratio is 2.43. We measured leaf N content, which was 1.10 (SE 0.05) g m$^{-2}$. Assuming the base leaf nitrogen content for photosynthesis is 0.24 g m$^{-2}$ (Yin *et al.* 2011), the slope of $V_{cmax}$ and $V_{pmax}$ versus leaf N is 57.7 µmol and 140.3 µmol (g N)$^{-1}$ s$^{-1}$, respectively.

The estimated $g_{bs}$ clearly varied with leaf temperature, and this response can be well described by the peaked Arrhenius equation, Equation 4 (Fig. 6). The obtained parameters of Equation 4 are: $g_{bs25}$=2.87 mmol m$^{-2}$ s$^{-1}$, $E$=116.7 kJ mol$^{-1}$, $D$=264.6 kJ mol$^{-1}$, and $S$=0.86 kJ K$^{-1}$ mol$^{-1}$ (Table 2). These parameter values of the peaked Arrhenius equation predicted, according to Equation 5, 34 °C as the optimum temperature for $g_{bs}$.

If we set $g_{bs}$ independent of temperature, the obtained estimates from fitting to our data would be: $g_{m25}$=4.37 mol m$^{-2}$ s$^{-1}$, $g_{bs}$=4.53 mmol m$^{-2}$ s$^{-1}$, $V_{cmax25}$=52.7 µmol m$^{-2}$ s$^{-1}$, and $V_{pmax25}$=80.0 µmol m$^{-2}$ s$^{-1}$, with $R^2$=0.98 and rRMSE=13.3%. The obtained $g_{m25}$ increased by >3-fold, $V_{pmax25}$ decreased by 33%, and, therefore, the $V_{pmax25}$:$V_{cmax25}$ ratio dropped to 1.5 and may have been underestimated (see the Discussion). Furthermore, this $g_{bs}$ temperature-insensitive model statistically decreased the goodness of fit ($P$<0.001 based on the $F$-test).

If we use the original model of von Caemmerer and Furbank (1999) which predicts $A$ as the minimum of two limiting $A_{TT}$

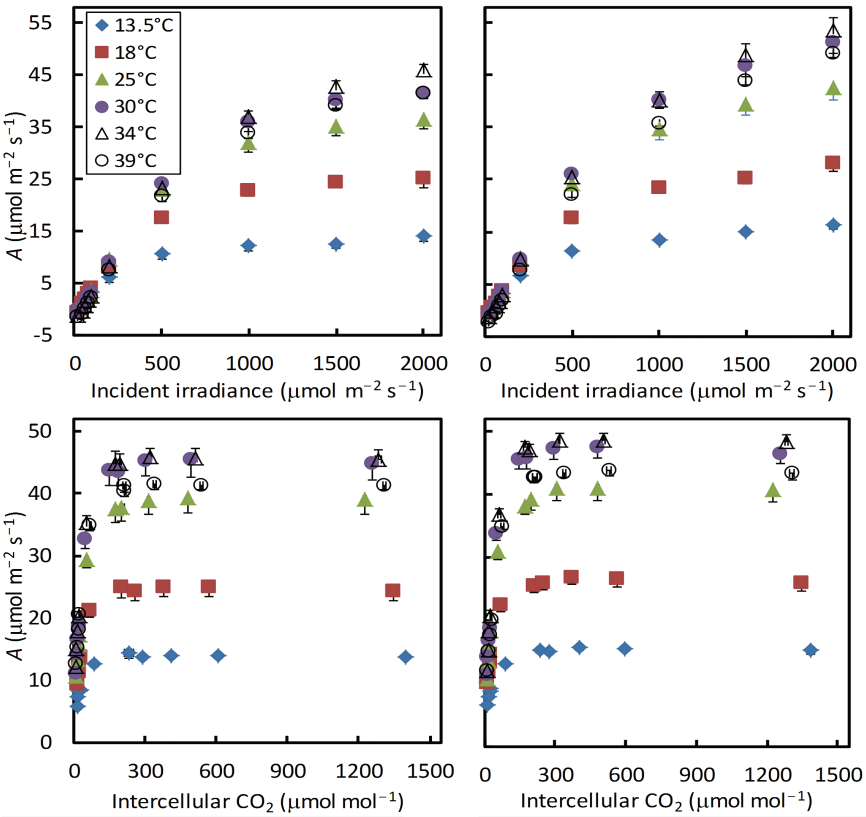


**Fig. 1.** Net $CO_2$ assimilation rate *A* at six leaf temperatures in response to incident irradiance or to intercellular $CO_2$ levels under 21% (left panels) or 2% (right panels) $O_2$ conditions. Each symbol represents the mean of four replicated leaves (SEMs are visible in bars if larger than the symbols).(This figure is available in colour at *JXB* online.)

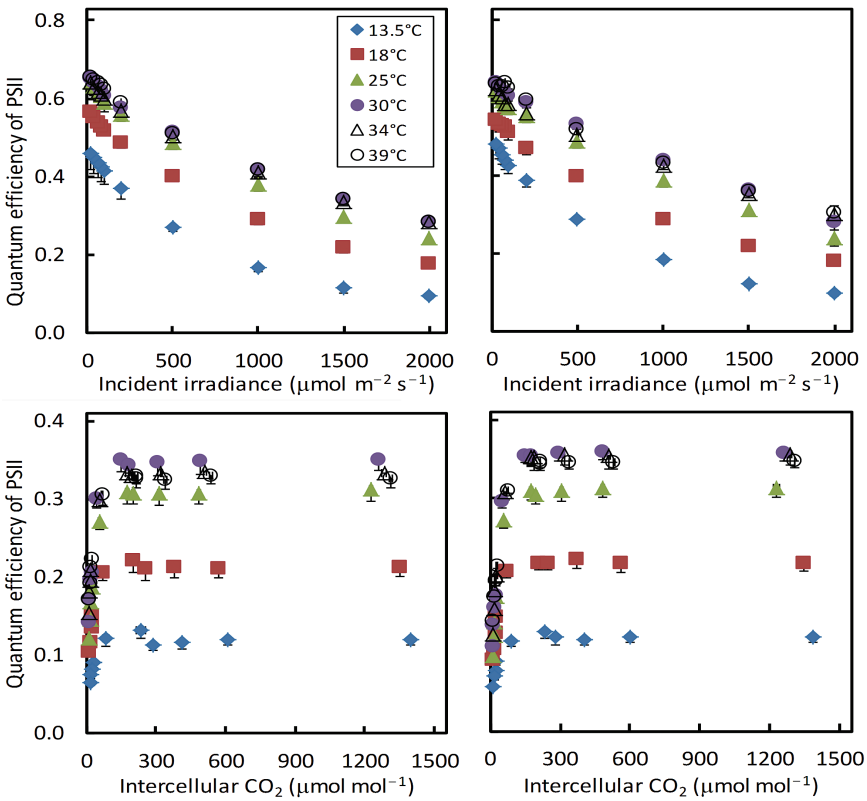


**Fig. 2.** Apparent operating quantum efficiency of photosystem II (PSII) electron transport ($\Phi_2$ or $\Delta F/F_m'$) at six leaf temperatures in response to incident irradiance or to intercellular $CO_2$ levels under 21% (left panels) or 2% (right panels) $O_2$ conditions. Each symbol represents the mean of four replicated leaves (SEMs are visible if larger than the symbols). (This figure is available in colour at *JXB* online.)

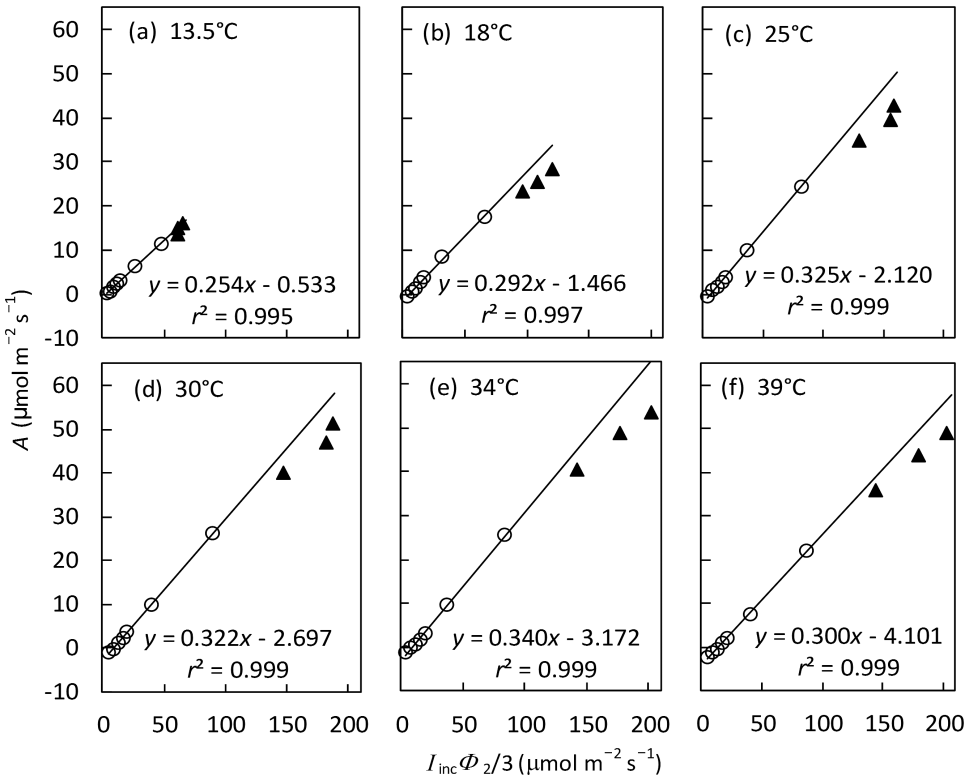


**Fig. 3.** The relationship between net $CO_2$ assimilation rate $A$ and the lumped variable $I_{inc}\Phi_2/3$ (mean of four replicates) from irradiance response curves under non-photorespiratory conditions (i.e. at 2% $O_2$ combined with high $CO_2$) at six leaf temperatures. Open circles are for $I_{inc}$ ≤500 μmol $m^{-2}$ $s^{-1}$ and filled triangles come from the three levels of $I_{inc}$ >500 μmol $m^{-2}$ $s^{-1}$. The lines represent linear regression based on data with $I_{inc}$ ≤500 μmol $m^{-2}$ $s^{-1}$, in which the slope gives the estimate of calibration factor $s'$ and the intercept gives the estimate of day respiration $R_d$ (see the text).

and $A_{EE}$, we obtained the estimates: $g_{m25}$=1.53 mol $m^{-2}$ $s^{-1}$, $V_{cmax25}$=41.9 μmol $m^{-2}$ $s^{-1}$, and $V_{pmax25}$=119.8 μmol $m^{-2}$ $s^{-1}$, with $g_{bs}$ being 1.18, 0.72, 3.39, 10.60, 9.35, and 5.07 mmol $m^{-2}$ $s^{-1}$ at 13.5, 18, 25, 30, 34, and 39 °C, respectively. The model described the data ($R^2$=0.97 and rRMSE=14.3%) somewhat less adequately than our four-rates model. Also, the estimates of $g_{bs}$ at 30 °C and 34 °C became higher, resulting in different parameter estimates for $g_{bs}$ temperature response: $g_{bs25}$=3.54 mmol $m^{-2}$ $s^{-1}$, $E$=264.9 kJ $mol^{-1}$, $D$=385.7 kJ $mol^{-1}$, and $S$=1.27 kJ $K^{-1}$ $mol^{-1}$. This gives $T_{opt}$=31.3 °C, ~2.6 °C lower than $T_{opt}$ resulting from the four-rates model. The difference stemmed from the fact that many data points were determined by $A_{TE}$ (results not shown), which is excluded in the two-rates model.

### *Sensitivity of estimated $g_{bs}$–temperature relationships to input parameters*

In Table 1, the value of $E_{Kp}$ was derived from our own data using an approximate model for describing the initial slope of $A$–$C_i$ curves (see earlier). This procedure may be criticized because (i) the approximate model assumes an infinite $g_m$; (ii) the procedure requires that the initial section of $A$–$C_i$ curves is exactly linear; and (iii) the required estimates for temperature response parameters of $V_{pmax}$, which we derived from Chinthapalli *et al.* (2003), may actually be uncertain. To examine the uncertainties in our estimated $E_{Kp}$, we used a more complete model (Supplementary appendix C) combined with two other reports (Massad *et al.*, 2007; Boyd *et al.*, 2015) on temperature response parameters of $V_{pmax}$. We fitted the model to the initial section of $A$–$C_i$ curves where $A$ is expected to be limited by the PEPc activity, and the obtained $E_{Kp}$ estimate was 66.3, 79.5, and 73.3 kJ $mol^{-1}$ if temperature response parameters of $V_{pmax}$ came from Chinthapalli *et al.* (2003), Massad *et al.* (2007), and Boyd *et al.* (2015), respectively (Supplementary Table S1). When the $E_{Kp}$ estimate was combined with their corresponding temperature response parameter values of $V_{pmax}$ from the three studies, the resulting estimates of $g_{bs}$ at six temperatures and of $V_{cmax25}$ were hardly affected by the use of these different sets of input for $E_{Kp}$ and temperature response of $V_{pmax}$ (Supplementary Table S1).

The temperature responses of $g_m$ do not yet exist for $C_4$ species, and temperature responses for $C_3$ species differed greatly among reports for tobacco (Bernacchi *et al.*, 2002; Evans and von Caemmerer, 2013; Walker *et al.*, 2013), and among species (von Caemmerer and Evans, 2015), in particular between tobacco and Arabidopsis (Walker *et al.*, 2013). The responses for tobacco ranged from the peaked Arrhenius response (Bernacchi *et al.*, 2002; Walker *et al.*, 2013) to a linear pattern (Evans and von Caemmerer, 2013), whereas data of Walker *et al.* (2013) for Arabidopsis showed virtually no effect of temperature on $g_m$. Despite such a contrast in the temperature response of $g_m$ used as input, the overall response of $g_{bs}$ to temperature remained similar, following a peaked Arrhenius pattern (Supplementary Fig. S3). The obtained $V_{cmax25}$ varied little, from 48.5 μmol $m^{-2}$ $s^{-1}$ to 51.4 μmol $m^{-2}$ $s^{-1}$. The obtained $V_{pmax25}$ varied to a greater extent, from 75.3 μmol $m^{-2}$ $s^{-1}$ (from using the Arabidopsis response) to 155.6 μmol

$m^{-2}$ $s^{-1}$ (from using the tobacco response of Walker *et al.*, 2013). The obtained $g_{m25}$ was mostly between 1.25 mol $m^{-2}$ $s^{-1}$ and 1.45 mol $m^{-2}$ $s^{-1}$, but using the Arabidopsis response gave an infinite estimate of $g_{m25}$.

For sensitivity analyses of the estimated $g_{bs}$ temperature response to 12 other parameters, the input parameters were varied by ±25% and 50% of their default values (Fig. 7). The estimated temperature response of $g_{bs}$ was least sensitive to changes in $K_p$ (Fig. 7a), $E_{KmO}$ (Fig. 7h), and $E_{Vpmax}$ (Fig. 7i). Overall, the sensitivity depended on the level of the parameter changes. Using extreme values of $\gamma^*_{25}$, $E_{Vcmax}$, $E_{\gamma^*}$, $E_{KmC}$, $D_{Vpmax}$, and $E_{Kp}$ changed the shape of the response, from the peaked optimum response to the non-peaked Arrhenius pattern. The −50% change in $D_{Vpmax}$ and +25% and +50% changes in $S_{Vpmax}$ resulted in a biologically unrealistic (negative) estimate of $g_{bs}$, so their resulting response pattern is not given (Fig. 7j, k), suggesting that these changes may have reached beyond biologically realistic scopes of the two parameters. Note that Equation 5 suggests a co-determination of $T_{opt}$ by $E$, $D$, and $S$ and a much higher sensitivity to $D_{Vpmax}$ and $S_{Vpmax}$ than to $E_{Vpmax}$ in determining $T_{opt}$ of $V_{pmax}$.

The ±25% and 50% changes of the 12 parameters also resulted in changes in estimated $g_{m25}$, $V_{cmax25}$, and $V_{pmax25}$ (results not shown). Overall, the estimated $V_{cmax25}$ varied least (from 45.7 µmol $m^{-2}$ $s^{-1}$ to 58.4 µmol $m^{-2}$ $s^{-1}$), and its relative change, defined as the difference between its maximum and minimum divided by its mean, was 26%, whereas $V_{pmax}$ varied most (from

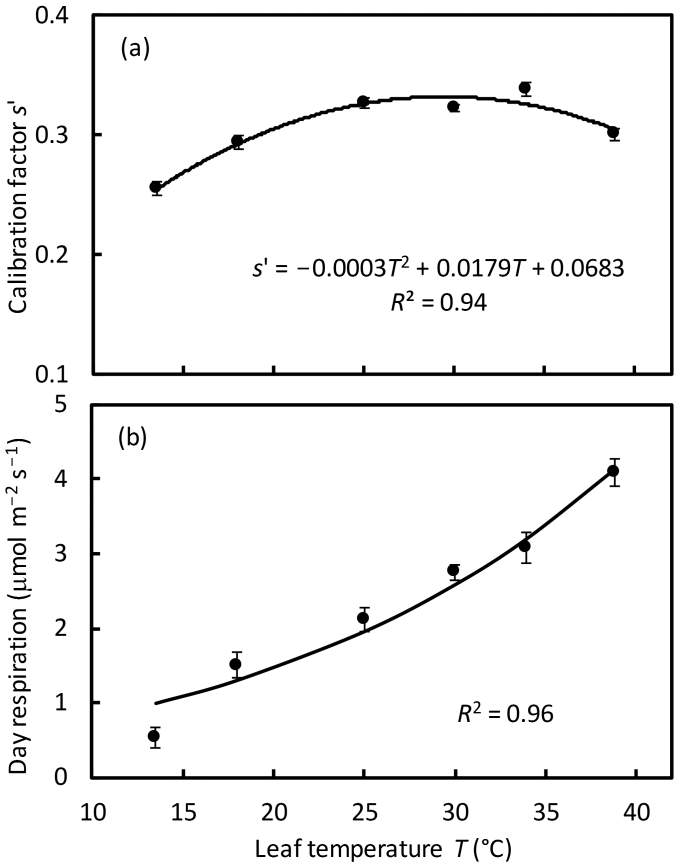


**Fig. 4.** (a) Temperature response of the estimated calibration factor $s'$, and (b) temperature response of the estimated day respiration $R_d$. Values of $s'$ and $R_d$ were estimated as the slope and the intercept, respectively, of linear regression in Fig. 3. In (b), the curve represents the Arrhenius plot of Equation 3 with estimated parameter values in Table 2. Bars in (a) and (b) represent SEs of the estimates.

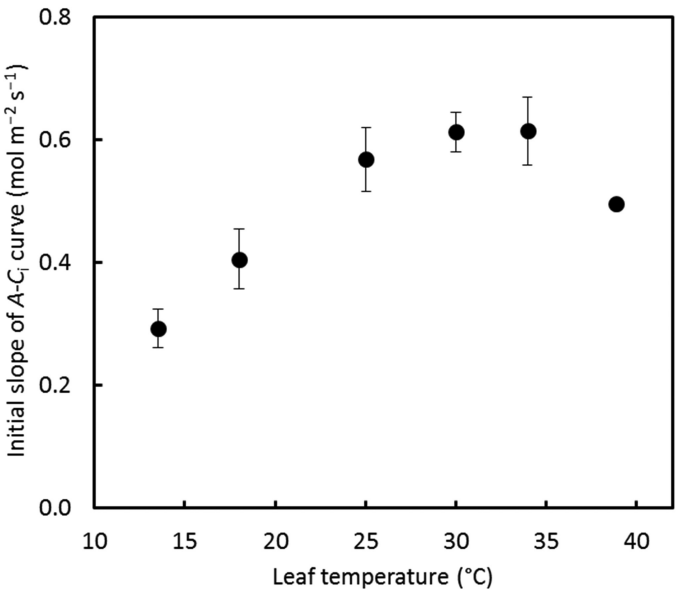


**Fig. 5.** Temperature response of the initial slope of the $A$–$C_i$ curve at 2% $O_2$. The error bar of each point indicates ±SEM of four replicated leaves. The error bar of the last point is smaller than the symbol.

**Table 2.** *Values (standard errors of the estimates in parentheses) of parameters at the reference temperature 25 °C, activation energy E in Equation 3 for day respiration ($R_d$), as well as activation energy E, deactivation energy D, and entropy term S of Equation 4 for bundle-sheath conductance ($g_{bs}$) and its optimum temperature $T_{opt}$ calculated from Equation 5, of maize leaves, as estimated from data in the present study*

| Parameter | Estimate at 25 °C | $E$ (kJ $mol^{-1}$) | $D$ (kJ $mol^{-1}$) | $S$ (kJ $K^{-1}$ $mol^{-1}$) | $T_{opt}$ (°C) |
|---|---|---|---|---|---|
| $R_d$ | 1.95(0.14) µmol $m^{-2}$ $s^{-1}$ | 41.85 (5.32) | NA | NA | NA |
| $g_m$ | 1.33(0.06) mol $m^{-2}$ $s^{-1}$ | – | – | – | – |
| $V_{cmax}$ | 49.0(0.9)µmol $m^{-2}$ $s^{-1}$ | – | NA | NA | NA |
| $V_{pmax}$ | 119.2(4.1)µmol $m^{-2}$ $s^{-1}$ | – | – | – | – |
| $g_{bs}$ | 2.87(0.31) mmol $m^{-2}$ $s^{-1}$ | 116.77 (30.39) | 264.60 (51.96) | 0.86 (0.16) | 33.9 |

NA, not applicable; –, not estimated from data of the present study, and most of them are given in Table 1, based on data in the literature, and were used as input to our present model analysis.

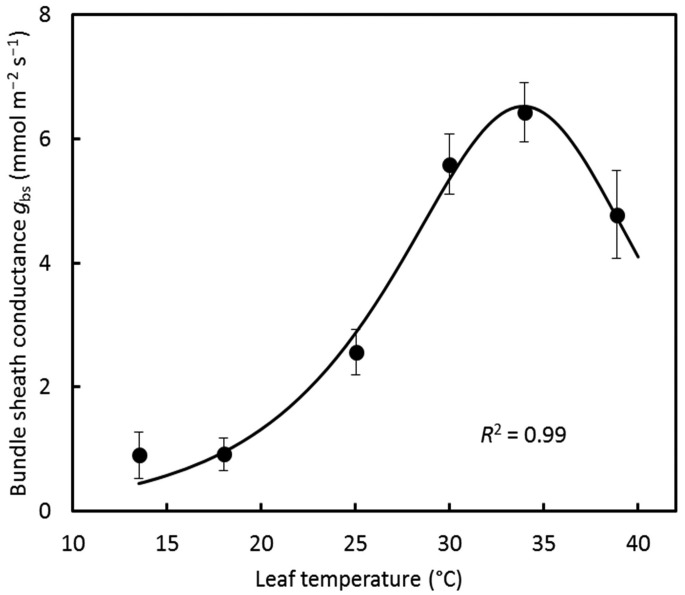


**Fig. 6.** Temperature response of estimated bundle-sheath conductance $g_{bs}$ in maize leaves. The error bar at each point represents ±SE of the estimate. The curve represents the peaked Arrhenius fit of Equation 4 with estimated values of the parameters in Table 2.

67.6 μmol m$^{-2}$ s$^{-1}$ to 322.6 μmol m$^{-2}$ s$^{-1}$), and its relative change was 195%. The relative change of the estimated $g_{m25}$ was 92% (from 0.93 mol m$^{-2}$ s$^{-1}$ to 2.05 mol m$^{-2}$ s$^{-1}$).

### *Estimated leakiness, and $V_o$:$V_c$ and $V_c$:$V_p$ ratios*

When model parameters are estimated, one can solve for leakiness ϕ (=$L/V_p$), $V_o$:$V_c$, and $V_c$:$V_p$ ratios, using Equations A1–A6 in Supplementary appendix A. The calculated ϕ declined sharply with increasing irradiance (Fig. 8a), and increased initially and then saturated with increasing $C_i$ (Fig. 8b). At low irradiances, ϕ values were very high, even exceeding 1.0 when the temperature was >30 °C (Fig. 8a). The temperature response of ϕ did not vary with $CO_2$ levels but depended strongly on the irradiance levels (Fig. 8c). The estimated ϕ at high irradiance (2000 μmol m$^{-2}$ s$^{-1}$) and the average ϕ of various $CO_2$ levels showed a peaked response to temperature (Fig. 8c).

The calculated $V_o$:$V_c$ ratio varied slightly with irradiance (Fig. 9a), and initially declined sharply and then became stable with increasing $CO_2$ levels (Fig. 9b). In accordance with this pattern, the $V_c$:$V_p$ ratio responded to irradiance and $CO_2$ levels (Fig. 9c, d). The $V_c$:$V_p$ ratio was <1.0 across irradiances (Fig. 9c), and it was also <1.0 for most $CO_2$ levels but became >1.0 at low $C_i$ of 10–30 μmol mol$^{-1}$, especially at high temperatures (Fig. 9d). Excluding the four low $CO_2$ levels, the average ratios were calculated to show how these ratios under normal irradiance and $CO_2$ conditions responded to temperature (inset in each panel of Fig. 9). Overall, the $V_o$:$V_c$ ratio increased with temperature (insets in Fig. 9a, b), and the $V_c$:$V_p$ ratio had a non-linear response to temperature (insets in Fig. 9c, d).

## Discussion

To estimate $g_{bs}$, we used the model method of Yin *et al.* (2011), which is based on the combined measurements of gas exchange and chlorophyll fluorescence on leaves. There are some concerns about this technique as the distribution of e$^-$ transport between mesophyll and bundle-sheath cells on $C_4$ leaves is uncertain (von Caemmerer, 2013; Kromdijk *et al.*, 2014). The mesophyll and bundle-sheath cells have different chloroplast populations which could result in a complex relationship between $\Delta F/F_m'$ and the quantum yield of $CO_2$ fixation. However, despite a few exceptions (e.g. Fryer *et al.*, 1998; Dwyer *et al.*, 2007), most studies (e.g. Krall and Edwards, 1990; Edwards and Baker, 1993; Oberhuber and Edwards, 1993; Oberhuber *et al.*, 1993; Peterson, 1994; Earl and Tollenaar, 1998; Laisk and Edwards, 1998; Siebke *et al.*, 2003; Naidu and Long, 2004; Loriaux *et al.*, 2013; Bellasio and Griffiths, 2014) have reported a good linear relationship for $C_4$ species between (quantum yields of) PSII e$^-$ transport from fluorescence analysis and $CO_2$ fixation from gas exchange data over a wide range of conditions. This empirical evidence suggests that combined gas exchange and chlorophyll fluorescence measurements, commonly applied to estimate $C_3$ photosynthesis parameters, can be similarly applied for $C_4$ photosynthesis, as implemented by Yin *et al.* (2011), Bellasio and Griffiths (2013, 2014), and Bellasio *et al.* (2016). The way we conducted calibrations using non-photorespiratory measurements to derive $s'$ for calculating $J_{atp}$ may also have reduced the uncertainty of applying a chlorophyll fluorescence technique to $C_4$ leaves.

In fact, the estimate of $s'$ is not just a calibration factor, but has physiological meanings and integrates a number of hard to determine parameters (Yin *et al.*, 2011):

$$s' = (1-x)\beta\rho_2 z\xi \tag{6}$$

where β is absorptance by leaf photosynthetic pigments, $\rho_2$ is the fraction of absorbed irradiance partitioned to PSII, $z$ is the factor of converting PSII e$^-$ flux into ATP flux, and ξ is the ratio of true PSII efficiency to fluorescence-measured apparent PSII efficiency. Theoretically, $\rho_2$ and $z$ can be written as (Yin and Struik. 2012):

$$\rho_2 = \frac{1-f_{cyc}}{(1-f_{cyc})+\Phi_{2LL}/\Phi_{1LL}} \tag{7}$$

$$z = \frac{2+f_Q-f_{cyc}}{h(1-f_{cyc})} \tag{8}$$

where $f_{cyc}$ is the fraction of e$^-$ flux at PSI that follows cyclic transport, $f_Q$ is the fraction of e$^-$ flux at reduced plastoquinone that follows the Q cycle, $h$ is the H$^+$:ATP ratio, and $\Phi_{2LL}/\Phi_{1LL}$ is the PSII:PSI e$^-$ transport efficiency ratio. Given recent quantitative estimation that $\Phi_{2LL}/\Phi_{1LL}$= ~0.825, $f_Q$=1, $f_{cyc}$= ~0.45, and $h$=4 (Yin and Struik, 2012), and assuming that $x$=0.4, β=0.9, and ξ=1, the value of $s'$ must be ~0.25. This theoretical value is close to our estimates for $s'$, 0.25–0.34 (Figs 3, 4a). Combining Equations 6–8 with the equation of Yin and Struik (2012) for the condition that the produced NADPH and ATP from e$^-$ transport match the metabolic requirements (their equation 5), $s'$ can also be expressed as:

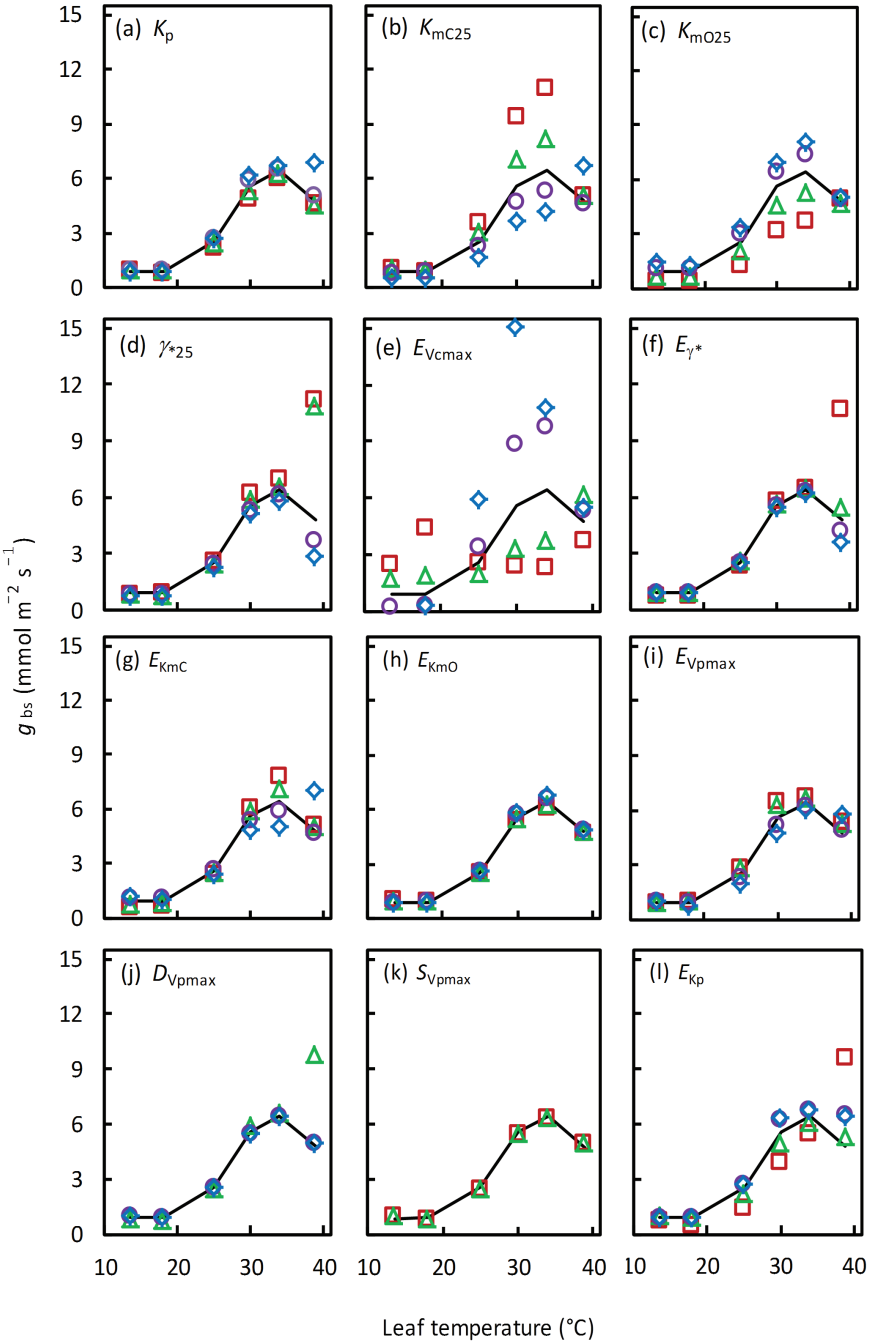


**Fig. 7.** Sensitivity of bundle-sheath conductance, $g_{bs}$, temperature response to changes in 12 input parameters as shown in (a–l). The input parameters and their default values are defined in Table 1. The changes were made to be 0.50 (open squares), 0.75 (open triangles), 1.25 (open circles), and 1.50 (open diamonds) times their default value. The temperature response of $g_{bs}$ using the default set of input parameter values is given by the solid curve of each panel. One or two types of symbols are missing in (j) and (k) because extreme values of either $D_{Vpmax}$ or $S_{Vpmax}$ resulted in a biologically unrealistic negative estimate of $g_{bs}$. (This figure is available in colour at *JXB* online.)

$$s' = \frac{3}{4}\beta\rho_2\xi(1+x\phi)\left(1-\frac{f_{pseudo}}{1-f_{cyc}}\right) \quad (9)$$

where $\phi$ is leakiness, $f_{pseudo}$ is the fraction of $e^-$ flux at PSI that follows the basal pseudocyclic transport (e.g. nitrate reduction, and malate export from chloroplasts), and the term $[1-f_{pseudo}/(1-f_{cyc})]$ as a whole refers to the fraction of the PSII $e^-$ flux that is used for supporting the Calvin circle and any photorespiration (Yin and Struik, 2012). Therefore, our calibration factor $s'$ takes into account only the part of the fluorescence signal dedicated to $e^-$ sinks represented by the Calvin cycle, any photorespiration, and some energy loss due to $CO_2$ leakage. Our calibration procedure has excluded the effect of possible basal alternative $e^-$ sinks. For example, the calibration factor $s'$ was found to vary with temperature (Fig. 4a), and one possible reason for this variation is that the extent of any basal alternative $e^-$ transport may depend on temperature.

Kromdijk *et al.* (2010) and Ubierna *et al.* (2013) estimated $g_{bs}$ by fitting the model of von Caemmerer and Furbank

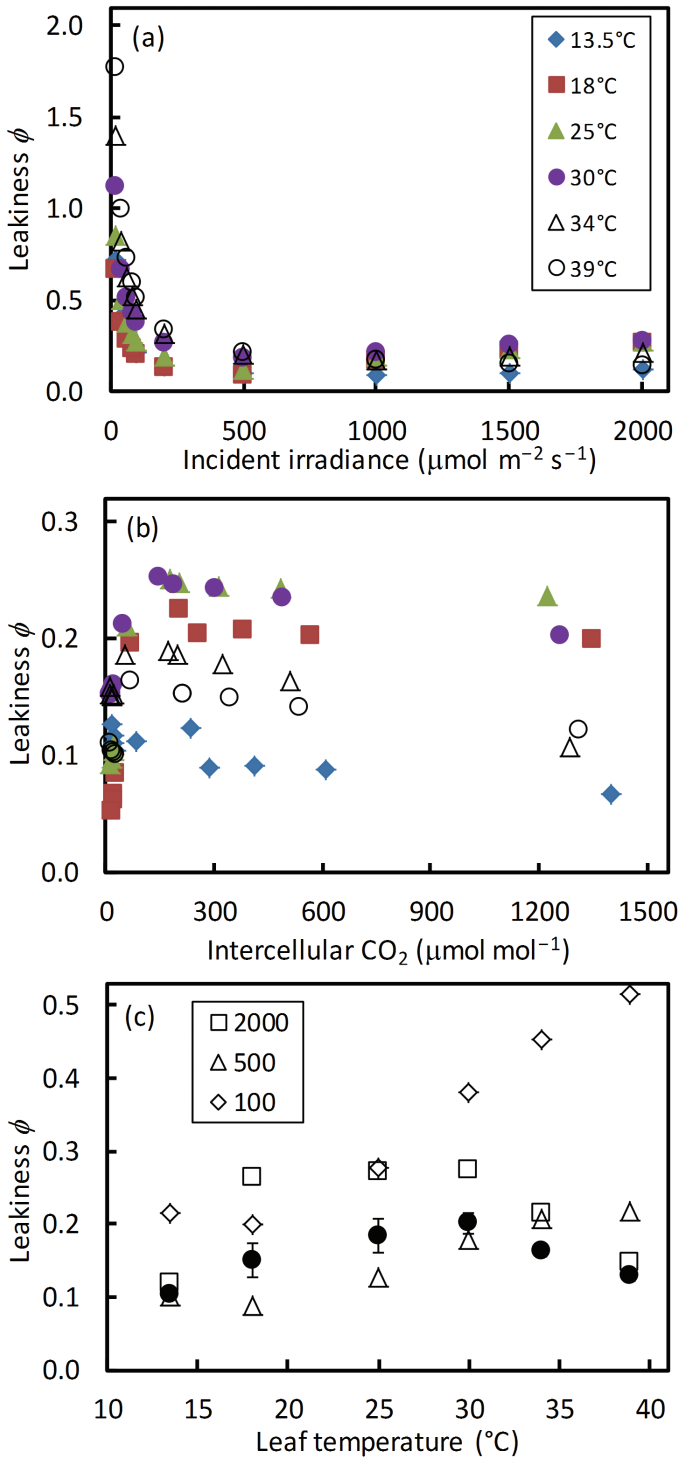


**Fig. 8.** Calculated $CO_2$ leakiness ϕ as a function of irradiance (a) and of intercellular $CO_2$ level (b) at six temperatures. The values of leakiness ϕ from (a) for three contrasting irradiance levels of 100, 500, and 2000 µmol $m^{-2}$ $s^{-1}$ (open symbols) and the mean ϕ (SEM in bars) across all $CO_2$ levels from (b) (filled circles) are shown as a function of temperature (c). The $O_2$ level was at 21%.(This figure is available in colour at *JXB* online.)

(1999) to carbon isotope discrimination data that were measured simultaneously with gas exchange, thereby providing an independent method to estimate $g_{bs}$. As this isotopic method has more assumptions than the fluorescence-based method (Kromdijk *et al.*, 2014) and does not estimate $J_{atp}$ and $R_d$, Bellasio and Griffiths (2013) compared the two methods in estimating $g_{bs}$ by using $J_{atp}$ and $R_d$ estimated along the lines of our method. It is noteworthy that the fluorescence method used by Bellasio and Griffiths (2013) slightly differs from our method in that they estimated $g_{bs}$ by minimizing the difference between modelled and measured $J_{atp}$, whereas our fitting method is to minimize the difference between modelled and measured $A$. Yin and Struik (2009*b*) have shown for $C_3$ photosynthesis that the two minimizing targets can result in slightly different estimates of $g_m$, and we prefer our method because it is generally $A$, rather than $J_{atp}$, that is to be predicted from the general use of photosynthesis models. Nevertheless, Bellasio and Griffiths (2013) found that, compared with $g_{bs}$ estimated by the isotopic method, $g_{bs}$ estimated by the fluorescence method by fitting to $J_{atp}$ was similar for maize leaves grown under low light conditions but was much lower for leaves from high light conditions; and the reasons for the difference are unresolved (Kromdijk *et al.*, 2014). Bellasio and Griffiths (2013) discussed several advantages of the fluorescence method compared with the isotopic method (e.g. lower noise/signal ratio). However, since the isotopic method does not have the same problem as the fluorescence method in dealing with the two cell types, it is necessary to study further whether the relative temperature response of $g_{bs}$ we obtained here (Figs 6, 7) can be confirmed using the independent isotopic method.

Our model considered only two major enzymes (i.e. PEPc for the $C_4$ cycle and Rubisco for the $C_3$ cycle). Other enzymes [e.g. pyruvate orthophosphate dikinase, $C_4$-acid decarboxylase, and carbonic anhydrase (CA)] are also important. The fact that detailed kinetic constants of these enzymes are rare and uncertain forces us to consider only two enzymes as in most applications of the $C_4$ model of von Caemmerer and Furbank (1999). Even for these two enzymes, only *in vitro* estimates of kinetic constants were used here as their *in vivo* estimates are practically impossible to obtain, and, when estimated, possibly confounded by the assumptions made on other parameters. For example, Massad *et al.* (2007) assumed that $g_{bs}$ and γ* are independent of temperature, and obtained *in vivo* estimates of the peaked Arrhenius temperature response (i.e. Equation 4) for $V_{cmax}$ and $V_{pmax}$, with $T_{opt}$=32.5°C and 43.3 °C, respectively. Their $T_{opt}$ estimate for $V_{pmax}$ is similar to our estimate of 44.4 °C based on *in vitro* data of Chinthapalli *et al.* (2003). However, the peaked temperature response for $V_{cmax}$ has seldom been observed *in vitro*, for both $C_3$ and $C_4$ Rubisco, even when the temperature is up to 35–40 °C (e.g. Badger and Collatz, 1977; Jordan and Ogren, 1984; Sage, 2002; Kubien *et al.*, 2003; Walker *et al.*, 2013; Boyd *et al.*, 2015; Perdomo *et al.*, 2015). We believe that the low $T_{opt}$ for $V_{cmax}$ obtained by Massad *et al.* (2007) could simply be because they ignored the temperature sensitivity of $g_{bs}$ and γ* when estimating $V_{cmax}$.

Our analysis showed the necessity of accounting for temperature response of $g_{bs}$. The shape of our temperature response of $g_{bs}$ using default parameters (Fig. 6) followed an optimum temperature response pattern of light- and $CO_2$-saturated photosynthesis rates ($A_{max}$), similar to that Bernacchi *et al.* (2002) and others obtained for $g_m$ in $C_3$ leaves. The similar temperature response of $g_m$ and $A_{max}$ is expected as $g_m$

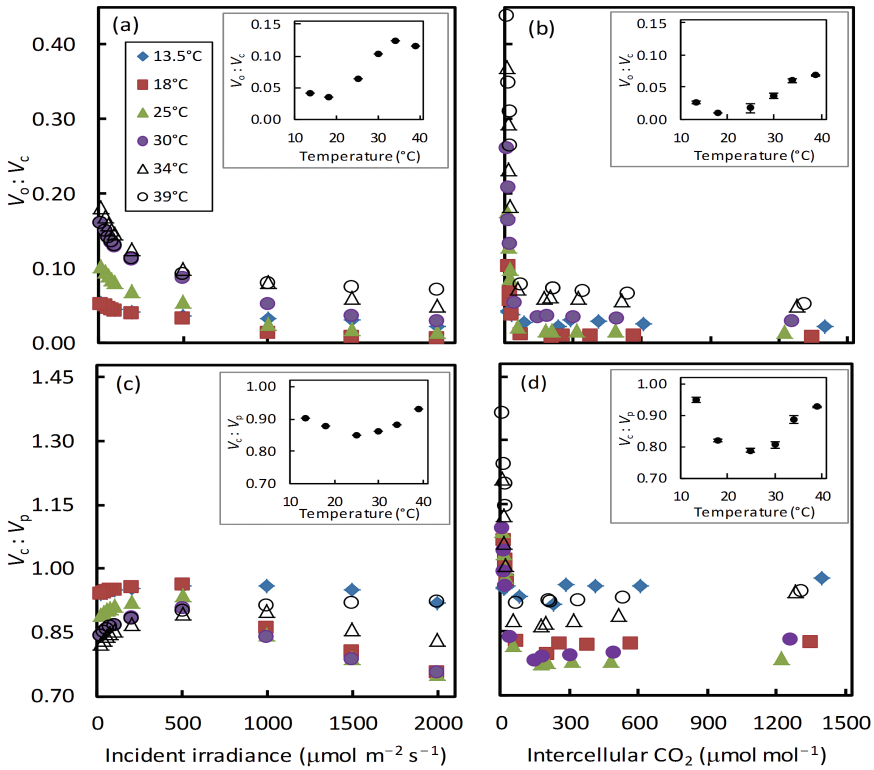


**Fig. 9** Calculated $V_o$:$V_c$ ratios (a, b) and $V_c$:$V_p$ ratios (c, d) as a function of irradiance (a, c) and of intercellular $CO_2$ level (b, d) at six temperatures. The mean ratios (SEM in bars if larger than symbols) across all irradiance levels and across $CO_2$ levels with $C_a$ ≥200 μmol mol$^{-1}$ against temperature during measurements are shown in the inset of each panel. The $O_2$ level was 21%.(This figure is available in colour at *JXB* online.)

positively affects $A_{max}$. The similar temperature response of $g_{bs}$ and $A_{max}$ found here is unexpected, as $g_{bs}$ negatively affects $A_{max}$ in $C_4$ leaves. Nevertheless, given the uncertainties in all input parameters we used, our result on the temperature response of $g_{bs}$ (Fig. 6) should be considered as tentative, and, as already stated, needs confirmation by other independent techniques. Our sensitivity analysis showed that the estimated temperature response of $g_{bs}$ depended only slightly on the assumed temperature response of $g_m$ (Supplementary Fig. S3), but more on Rubisco and PEPc kinetic parameters (Fig. 7). Using extreme values of some kinetic parameters occasionally caused a change from an optimum response to an accelerating response to temperature (Fig. 7). The $g_{bs}$ temperature response rarely depends on $g_m$ parameters but more on Rubisco and PEPc kinetic parameters; this is expected from the model of von Caemmerer and Furbank (1999), because the calculation of $C_c$ is minimally affected by $g_m$ through $C_m$, and $V_c$ depends strongly on $g_{bs}$ and $V_{cmax}$. However, those kinetics parameters to which the estimated temperature response of $g_{bs}$ is very sensitive were either measured for maize (e.g. $K_{mC25}$, $K_{mO25}$,and $\gamma^*_{25}$, reported by Cousins *et al.*, 2010) or were relatively conserved among $C_4$ species ($E_{Vcmax}$ and $E_{\gamma^*}$; see above). Also uncertainties related to a set of PEPc kinetics parameters as a whole had little impact on $g_{bs}$ estimates (Supplementary Table S1), although individual parameters such as $D_{Vpmax}$ and $S_{Vpmax}$—when varied independently—strongly influenced the estimated $g_{bs}$ (Fig. 7). Despite these uncertainties of the input parameters, the obtained $g_{bs}$–$T_{leaf}$ relationship between 13.5 °C and 39.0 °C followed either a peaked or non-peaked Arrhenius pattern (Figs 6, 7). Below 35 °C, the estimated $g_{bs}$ almost exclusively increased monotonously with increasing temperature (Fig. 7). The activation energy estimate based on Equation 3 for our estimates of $g_{bs}$ in Fig. 6 within 35 °C was ~74.45 kJ mol$^{-1}$ for our study, and its corresponding $Q_{10}$ value was ~2.74.

The $Q_{10}$ factor for diffusion of $CO_2$ in water is ~1.25 (Bernacchi *et al.*, 2002). Our higher $Q_{10}$ value for $g_{bs}$ suggests the possibility that some proteins/enzymes are involved in inter- and intracellular $CO_2$ diffusion in $C_4$ leaves. One candidate is CA, which facilitates the $CO_2$ diffusion rate (Badger and Price, 1994). CA has often been considered to play a role in mediating $g_m$ in $C_3$ species (e.g. Bernacchi *et al.*, 2002). Its role for $g_m$ in $C_4$ leaves is justified since in $C_4$ plants CA is mainly found in the cytosol alongside PEPc (Ludwig *et al.*, 2011), and CA activity is temperature dependent (Boyd *et al.*, 2015). This actually gives indirect support to the use of the modified Arrhenius response for the temperature effect on $g_m$ in our analysis. The bundle-sheath cells may contain some amount of CA isoforms (Ludwig *et al.*, 2011), seemingly in support of its potential mediating role for $g_{bs}$ as well. The other candidate may be an aquaporin that increases the $CO_2$ permeability of the cell membrane (Terashima and Ono, 2002). Genetic manipulation of specific aquaporins has been used to vary $g_m$ in $C_3$ species (e.g. Hanba *et al.*, 2004). Brautigam *et al.* (2010) showed that a 20-fold up-regulation in the abundance of an mRNA coding for an aquaporin was registered in a $C_4$ species. Other temperature-dependent activities may also shape our observed $g_{bs}$–temperature

relationship. For example, the current model simply assumes that the rate of decarboxylation equals $V_p$. Recently it has been suggested that maize leaves have mixed decarboxylation pathways (Furbank, 2011). Theoretical modelling by Wang *et al.* (2014) showed that engaging the mixed pathways could decrease the need to maintain a high concentration gradient of metabolites between mesophyll and bundle-sheath cells, reconciling an earlier analysis of Sowinski *et al.* (2008) that simple diffusion-driven transport of metabolites is not adequate to explain the metabolite exchange during $C_4$ photosynthesis. The mixed decarboxylation pathways and associated cell to cell exchange of metabolites suggest it likely that PEPc carboxylation and the overall decarboxylation rates are not the same and have different temperature responses. In that case, such a difference will have been lumped with our estimated parameters for temperature response of $g_{bs}$.

The temperature response of $g_{bs}$, together with the temperature responses of $J_{atp}$, Rubisco, and PEPc kinetic parameters, co-determined the temperature responses of leakiness $\phi$ (Fig. 8), and $V_o$:$V_c$ and $V_c$:$V_p$ ratios (Fig. 9). In line with the trends shown by theoretical modelling (von Caemmerer and Furbank, 1999) and experimental calculation (Kromdijk *et al.*, 2010; Pengelly *et al.*, 2010; Yin *et al.*, 2011; Ubierna *et al.*, 2013; Bellasio and Griffiths, 2014), the calculated $\phi$ declined sharply with increasing irradiance (Fig. 8a). However, $\phi$ at low irradiances even exceeded 1.0 when the temperature was above 30 °C (Fig. 8a). The extreme $\phi$ values >1 at strictly limiting irradiances and high temperatures resulted from relatively high mitochondrial respiration in bundle-sheath cells combined with relatively high photorespiratory rates (as indicated by relatively high $V_o$:$V_c$ ratios at low irradiances; Fig. 9a). As a result, the temperature response of $\phi$ did not vary with $CO_2$ levels but depended strongly on the irradiance levels (Fig. 8c). The estimated $\phi$ at high irradiances and the average $\phi$ of various $CO_2$ levels showed a flat peaked response to temperature (Fig. 8c), in line with the trend shown by von Caemmerer *et al.* (2014) with the carbon isotope method.

For an effective CCM, the $V_c$:$V_p$ ratio is expected to be <1.0. However, the $V_c$:$V_p$ ratio went up to >1.0 at low $CO_2$, especially at high temperatures (Fig. 9d). The model of von Caemmerer and Furbank (1999) (see Equations A1 and A4 in Supplementary appendix A) predicts that the $V_c$:$V_p$ ratio is ≥1.0 only if $L \leq 0.5V_o+(R_d-R_m)$. This condition was met at our four lowest $CO_2$ levels ($C_i$ of 10–30 μmol mol$^{-1}$) where $V_o$ was high. The average ratios under normal irradiance and $CO_2$ conditions (calculated by excluding those four low $CO_2$ levels) responded to temperature. Overall, the $V_o$:$V_c$ ratio increased with temperature (insets in Fig. 9a, b), because increasing temperature favoured the RuBP oxygenation relative to carboxylation. However, this general temperature response of the $V_o$:$V_c$ ratio seemed to be modified by the temperature response of $g_{bs}$. The temperature response of $g_{bs}$ and its associated temperature response of leakiness (Fig. 8c) required $V_p$ to vary accordingly, resulting in a non-linear response of the $V_c$:$V_p$ ratio to temperature (insets in Fig. 9c, d).

Our parameter estimates can be compared with previous literature reports. Our estimate of activation energy for $R_d$, 41.9 kJ mol$^{-1}$ (Table 2), is within the range of reports for $R_d$ in $C_3$ species (24.2–65.2 kJ mol$^{-1}$; see review by Yin *et al.*, 2014) as well as the range reported for $C_4$ species (28.2–57.8 kJ mol$^{-1}$; Dwyer *et al.* 2007). Our estimate for $g_{m25}$,1.33 mol m$^{-2}$ s$^{-1}$ (Table 2), is within the range of the earlier estimated or suggested values for maize (Pfeffer and Peisker, 1998; Kromdijk *et al.*, 2010; Yin *et al.*, 2011; Barbour *et al.*, 2016), and is higher than that for $C_3$ leaves (for which the maximum $g_{m25}$ is ~0.6 mol m$^{-2}$ s$^{-1}$; e.g. Loreto *et al.*, 1992). Our estimated $V_{pmax25}$:$V_{cmax25}$ ratio, 2.43, agrees with our earlier estimate 2.5 (Yin *et al.*, 2011). Biochemical measurements on this ratio were 2.1–2.5 (Pengelly *et al.*, 2010), 3.1 (Kubien *et al.*, 2003), or higher (Sage *et al.*, 1987). The leaf N content in our experiment was on average 1.1 g N m$^{-2}$. Our estimated $g_{bs25}$, 2.87 mmol m$^{-2}$ s$^{-1}$ (Table 2), is within the values reported for maize, 1.5 mmol m$^{-2}$ s$^{-1}$ (Ubierna *et al.*, 2013), 0.37–2.35 mmol m$^{-2}$ s$^{-1}$ (Kromdijk *et al.*, 2010), and 0.82–4.64 mmol m$^{-2}$ s$^{-1}$ (Bellasio and Griffiths, 2014), and also agrees with our previous estimate for this leaf nitrogen level (Yin *et al.*, 2011). However, our estimates for the slope of $V_{cmax25}$ and $V_{pmax25}$ versus leaf nitrogen, 57.7 μmol and 140.3 μmol (g N)$^{-1}$ s$^{-1}$, respectively, are lower than the previous estimates [96.0 μmol and 242.2 μmol (g N)$^{-1}$ s$^{-1}$, respectively] by Yin *et al.* (2011). The difference between the two studies in glasshouse environments (i.e. ~1 month later in the present study than in the previous study of Yin *et al.*, 2011), cultivars used ('Atrium' versus '2-02R10074'), and leaf ranks for measurements (the seventh versus the eighth to ninth) might have caused this disparity. It has been shown that acclimation to growing light intensities affected photosynthesis parameters in maize (Kromdijk *et al.*, 2010; Bellasio and Griffiths, 2013) and other $C_4$ species (Ubierna *et al.*, 2011).

Previously only one study (Kiirats *et al.*, 2002) has reported the temperature response of $g_{bs}$; that is, $g_{bs}$ increases almost linearly with increasing leaf temperature, in contrast to our result for the Arrhenius response. Their temperature was only up to 35 °C. If normalized to 25 °C, the response within temperatures up to 35 °C was still different between their study and ours (Supplementary Fig. S4): the activation energy estimate based on Equation 3 was ~24.92 kJ mol$^{-1}$ for their study, lower than 74.45 kJ mol$^{-1}$ for our study (see above). This may highlight species differences in temperature response of $g_{bs}$, although the impact of methodological differences between the two studies and/or the impact of uncertainty in input parameter values for our study cannot be ruled out. Temperature response of $g_m$ for $C_3$ photosynthesis has recently been reported to vary greatly with plant species (Walker *et al.*, 2013; von Caemmerer and Evans, 2015). There is a need to investigate further whether or not species diversity exists with regards to temperature response of $g_{bs}$ for $C_4$ photosynthesis. To that end, comprehensive investigations on enzyme kinetic constants may need to be carried out across contrasting $C_4$ species.

In short, our study demonstrates that in contrast to existing modelling assumptions, $g_{bs}$ does vary with leaf temperature. Although the presented temperature response curve still needs to be confirmed by other independent techniques, our results provide a step forward to more accurate modelling

of $C_4$ photosynthesis and productivity, especially for maize, under changing climatic environments.

## Supplementary data

Supplementary data are available at *JXB* online.

Appendix A. Basic equations in the $C_4$ photosynthesis model of von Caemmerer and Furbank (1999) and analytical solutions of the model as given by Yin *et al.* (2011).

Appendix B. Quantifying temperature dependence of diffusivities and solubilities of $CO_2$ and $O_2$ in water.

Appendix C. Model and data for describing PEPc-limited rates of photosynthesis within the initial section of $A$–$C_i$ curves.

Table S1. Estimated values of $E_{Kp}$, $V_{cmax25}$, and $g_{bs}$ at six temperatures when using three sets of $V_{pmax}$ parameters.

Figure S1. The initial linear section of $A$–$C_i$ curves of 2% $O_2$ at six measurement temperatures.

Figure S2. Comparison between modelled and measured $A$–$I_{inc}$ and $A$–$C_i$ curves at six leaf temperatures under the condition of 21% $O_2$.

Figure S3. Temperature response of bundle-sheath conductance, estimated using four contrasting temperature responses of mesophyll conductance.

Figure S4. Comparison of temperature response of bundle-sheath conductance normalized to 1.0 at 25 °C between Kiirats *et al.* (2002) for *Amaranthus edulis* and our study for maize.

## Acknowledgements

This research is financed in part by the BioSolar Cells open innovation consortium, supported by the Dutch Ministry of Economic Affairs, Agriculture and Innovation.

## References

**Badger MR, Collatz GJ.** 1977. Studies on the kinetic mechanism of ribulose-1,5-biophosphate carboxylase and oxygenase reactions, with particular reference to the effect of temperature on kinetic parameters. Carnegie Instute of Washington Yearbook **76,** 355–361.

**Badger MR, Price GD.** 1994. The role of carbonic anhydrase in photosynthesis. Annual Review of Plant Physiology and Plant Molecular Biology **45,** 369–392.

**Barbour MM, Evans JR, Simonin KA, von Caemmerer S.** 2016. Online $CO_2$ and $H_2O$ oxygen isotope fractionation allows estimation of mesophyll conductance in $C_4$ plants, and reveals that mesophyll conductance decreases as leaves age in both $C_4$ and $C_3$ plants. New Phytologist (in press).

**Bellasio C, Griffiths H.** 2013. Acclimation to low light by $C_4$ maize: implications for bundle sheath leakiness. Plant, Cell and Environment **37,** 1046–1058.

**Bellasio C, Griffiths H.** 2014. Acclimation of $C_4$ metabolism to low light in mature maize leaves could limit energetic losses during progressive shading in a crop canopy. Journal of Experimental Botany **65,** 3725–3736.

**Bellasio C, Beerling DJ, Griffiths H.** 2016. Deriving $C_4$ photosynthetic parameters from combined gas exchange and chlorophyll fluorescence using an Excel tool: theory and practice. Plant, Cell and Environmen t (in press).

**Bernacchi CJ, Portis AR, Nakano H, von Caemmerer S, Long SP.** 2002. Temperature response of mesophyll conductance. Implication for the determination of Rubisco enzyme kinetics and for limitations to photosynthesis *in vivo*. Plant Physiology **130,** 1992–1998.

**Bernacchi CJ, Singsaas EL, Pimentel C, Portis AR Jr, Long SP.** 2001. Improved temperature response functions for models of Rubisco-limited photosynthesis. Plant, Cell and Environment **24,** 253–259.

**Berry JA, Farquhar GD.** 1978. The $CO_2$-concentrating function of $C_4$ photosynthesis. A biochemical model. In Hall DO, Coombs J, Goodwin TW, eds, Proceedings of the 4th International Congress on Photosynthesis. London: Biochemical Society, 119–131.

**Boyd RA, Gandin A, Cousins AB.** 2015. Temperature response of $C_4$ photosynthesis: biochemical analysis of Rubisco, phospho*enol*pyruvate carboxylase and carbonic anhydrase in *Setaria viridis*. Plant Physiology **169,** 1850–1861.

**Brautigam A, Kajala K, Wullenweber J, *et al*.** 2010. An mRNA blueprint for $C_4$ photosynthesis derived from comparative transcriptomics of closely related $C_3$ and $C_4$ species. Plant Physiology **155,** 142–156.

**Chapman KSR, Berry JA, Hatch MD.** 1980. Photosynthetic metabolism in bundle sheath cells of the $C_4$ species *Zea mays*: sources of ATP and NADPH and the contribution of Photosystem II. Archives of Biochemistry and Biophysics **202,** 330–341.

**Chen D-X, Coughenour MB, Knapp AK, Owensby CE.** 1994. Mathematical simulation of $C_4$ grass photosynthesis in ambient and elevated $CO_2$. Ecological Modelling **73,** 63–80.

**Chinthapalli B, Murmu J, Raghavendra AS.** 2003. Dramatic difference in the response of phosphoenolpyruvate carboxylase to temperature in leaves of $C_3$ and $C_4$ plants. Journal of Experimental Botany **54,** 707–714.

**Collatz GJ, Ribas-Carbo M, Berry JA.** 1992. Coupled photosynthesis–stomatal conductance model for leaves of $C_4$ plants. Australian Journal of Plant Physiology **19,** 519–538.

**Cousins AB, Ghannoum O, von Caemmerer S, Badger MR.** 2010. Simultaneous determination of Rubisco carboxylase and oxygenase kinetic parameters in Triticum aestivum and Zea mays using membrane inlet mass spectrometry. Plant, Cell and Environment **33,** 444–452.

**Dwyer SA, Ghannoum O, Nicotra A, von Caemmerer S.** 2007. High temperature acclimation of $C_4$ photosynthesis is linked to changes in photosynthetic biochemistry. Plant, Cell and Environment **30,** 53–66.

**Earl H, Tollenaar M.** 1998. Relationship between thylakoid electron transport and photosynthetic $CO_2$ uptake in leaves of three maize (*Zea mays* L.) hybrids. Photosynthesis Research **58,** 245–257.

**Edwards GE, Baker NR.** 1993. Can assimilation in maize leaves be predicted accurately from chlorophyll fluorescence analysis? Photosynthesis Research **37,** 89–102.

**Evans JR, von Caemmerer S.** 2013. Temperature response of carbon isotope discrimination and mesophyll conductance in tobacco. Plant, Cell and Environment **36,** 745–756.

**Farquhar GD, von Caemmerer S, Berry JA.** 1980. A biochemical model of photosynthetic $CO_2$ assimilation in leaves of $C_3$ species. Planta **149,** 78–90.

**Frank MJW, Kuipers JAM, Vanswaaij WPM.** 1996. Diffusion coefficients and viscosities of $CO_2$ + $H_2O$, $CO_2$ + $CH_3OH$, $NH_3$ + $H_2O$, and $NH_3$ + $CH_3OH$ liquid mixtures. Journal of Chemical and Engineering Data **41,** 297–302.

**Fryer MJ, Andrews JR, Oxborough K, Blowers DA, Baker NR.** 1998. Relationship between CO2 assimilation, photosynthetic electron transport, and active $O_2$ metabolism in leaves of maize in the field during periods of low temperature. Plant Physiology **116,** 571–580.

**Furbank RT.** 2011. Evolution of the $C_4$ photosynthetic mechanism: are there really three $C_4$ acid decarboxylation types? Journal of Experimental Botany **62,** 3103–3208.

**Genty B, Briantais J-M, Baker N.** 1989. The relationship between the quantum yield of photosynthetic electron transport and quenching of chlorophyll fluorescence. Biochimica et Biophysica Acta **990,** 87–92.

**Han P, Bartels DM.** 1996. Temperature dependence of oxygen diffusion in $H_2O$ and $D_2O$. Journal of Physical Chemistry **100,** 5597–5602.

**Hanba YT, Shibasaka M, Hayashi Y, Hayakawa T, Kasamo K, Terashima I, Katsuhara M.** 2004. Overexpression of the barley aquaporin HvPIP2:1 increases internal $CO_2$ conductance and $CO_2$ assimilation in the leaves of transgenic rice plants. Plant and Cell Physiology **45,** 521–529.

**Hatch MD, Agostino A, Jenkins CLD.** 1995. Measurement of the leakage of $CO_2$ from bundle-sheath cells of leaves during $C_4$ photosynthesis. Plant Physiology **108,** 173–181.

**He D, Edwards GE.** 1996. Estimation of diffusive resistance of bundle sheath cells to $CO_2$ from modeling of $C_4$ photosynthesis. Photosynthesis Research **49,** 195–208.

**Heaton EA, Dohleman FG, Long SP.** 2008. Meeting US biofuel goals with less land: the potential of Miscanthus. Global Change Biology **14,** 2000–2014.

**Jordan DB, Ogren WL.** 1984. The $CO_2/O_2$ specificity of ribulose 1,5-biphosphate carboxylase/oxygenase: dependence on ribulose bisphosphate concentration, pH and temperature. Planta **161,** 308–313.

**Kiirats O, Lea PJ, Franceschi VR, Edwards GE.** 2002. Bundle sheath diffusive resistance to $CO_2$ and effectiveness of $C_4$ photosynthesis and refixation of photorespired $CO_2$ in a $C_4$ cycle mutant and wild-type *Amaranthus edulis*. Plant Physiology **130,** 964–976.

**Krall JK, Edwards GE.** 1990. Quantum yields of photosystem II electron transport and carbon fixation in $C_4$ plants. Australian Journal of Plant Physiology **17,** 579–588.

**Kromdijk J, Griffiths H, Schepers HE.** 2010. Can the progressive increase of $C_4$ bundle sheath leakiness at low PFD be explained by incomplete suppression of photorespiration? Plant, Cell and Environment **33,** 1935–1948.

**Kromdijk J, Ubierna N, Cousins AB, Griffiths H.** 2014. Bundle-sheath leakiness in $C_4$ photosynthesis: a careful balancing act between $CO_2$ concentration and assimilation. Journal of Experimental Botany **65,** 3443–3457.

**Kubien DS, von Caemmerer S, Furbank RT, Sage RF.** 2003. $C_4$ photosynthesis at low temperature. A study using transgenic plants with reduced amounts of Rubisco. Plant Physiology **132,** 1577–1585.

**Laisk A, Edwards GE.** 1998. Oxygen and electron flow in $C_4$ photosynthesis: Mehler reaction, photorespiration and $CO_2$ concentration in the bundle sheath. Planta **205,** 632–645.

**Leegood RC.** 2002. $C_4$ photosynthesis: principles of $CO_2$ concentration and prospects for its introduction into $C_3$ plants. Journal of Experimental Botany **53,** 581–590.

**Leegood RC, von Caemmerer S.** 1989. Some relationships between contents of photosynthetic intermediates and the rate of photosynthetic carbon assimilation in leaves of Zea mays L. Planta **178,** 258–266.

**Loreto F, Harley PC, Di Marco G, Sharkey TD.** 1992. Estimation of mesophyll conductance to $CO_2$ flux by three different methods. Plant Physiology **98,** 1437–1443.

**Loriaux SD, Avenson TJ, Wells JM, McDermitt DK, Eckles RD, Riensche B, Genty B.** 2013. Closing in on maximum yield of chlorophyll fluorescence using a single multiphase flash of sub-saturating intensity. Plant, Cell and Environment **36,** 1755–1770.

**Ludwig M.** 2011. The molecular evolution of β-carbonic anhydrase in Flaveria. Journal of Experimental Botany **62,** 3071–3081.

**Massad R-S, Tuzet A, Bethenod O.** 2007. The effect of temperature on $C_4$-type leaf photosynthesis parameters. Plant, Cell and Environment **30,** 1191–1204.

**Medlyn BE, Dreyer E, Ellsworth D, *et al*.** 2002. Temperature response of parameters of a biochemically based model of photosynthesis. II. A review of experimental data. Plant, Cell and Environment **25,** 1167–1179.

**Naidu SL, Long SP.** 2004. Potential mechanisms of low-temperature tolerance of $C_4$ photosynthesis in *Miscanthus* × *giganteus*: an in vivo analysis. Planta **220,** 145–155.

**Oberhuber W, Dai Z-Y, Edwards GE.** 1993. Light dependence of quantum yields of photosystem II and $CO_2$ fixation in $C_3$ and $C_4$ plants. Photosynthesis Research **35,** 265–274.

**Oberhuber W, Edwards GE.** 1993. Temperature dependence of the linkage of quantum yield of photosystem II to $CO_2$ fixation in $C_4$ and $C_3$ plants. Plant Physiology **101,** 507–512.

**Ort DR, Long SP.** 2014. Limits on yields in the corn belt. Science **344,** 484–485.

**Pedomo JA, Cavanagh AP, Kubien DS, Galmes J.** 2015. Temperature dependence of *in vitro* Rubisco kinetics in species of *Flaveria* with different photosynthetic mechanisms. Photosynthesis Research **124,** 67–75.

**Pengelly JJL, Sirault XRR, Tazoe Y, Evans JR, Furbank RT, von Caemmerer S.** 2010. Growth of the $C_4$ dicot *Flaveria bidentis*: photosynthetic acclimation to low light through shifts in leaf anatomy and biochemistry. Journal of Experimental Botany **61,** 4109–4122.

**Peterson RB.** 1994. Regulation of electron transport in photosystems I and II in $C_3$, $C_3$–$C_4$, and $C_4$ species of *Panicum* in response to changing irradiance and $O_2$ levels. Plant Physiology **105,** 349–356.

**Pfeffer M, Peisker M.** 1995. *In vivo* $K_m$ for $CO_2$ ($K_p$) of phosphoenolpyruvate carboxylase (PEPC) and mesophyll $CO_2$ transport resistance ($r_m$) in leaves of *Zea mays* L. In: Mathis P, ed. Photosynthesis: from light to biosphere , Vol. **V**. Dordrecht, The Netherlands: Kluwer Academic Publishers, 547–550.

**Pfeffer M, Peisker M.** 1998. $CO_2$ gas exchange and phosphoenolpyruvate carboxylase activity in leaves of *Zea mays* L. Photosynthesis Research **58,** 281–291.

**Sage RF.** 2002. Variation in the $k_{cat}$ of Rubisco in $C_3$ and $C_4$ plants and some implications for photosynthetic performance at high and low temperature. Journal of Experimental Botany **53,** 609–620.

**Sage RF, Kubien DS.** 2007. The temperature response of $C_3$ and $C_4$ photosynthesis. Plant, Cell and Environment **30,** 1086–1106.

**Sage RF, Pearcy RW, Seamann JR.** 1987. The nitrogen use efficiency of $C_3$ and $C_4$ plants. III. Leaf nitrogen effects on the activity of carboxylating enzymes in *Chenopodium album* (L.) and *Amaranthus retroflexus* (L.). Plant Physiology **85,** 355–359.

**Scafaro AP, von Caemmerer S, Evans JR, Atwell BJ.** 2011. Temperature response of mesophyll conductance in cultivated and wild *Oryza* species with contrasting mesophyll cell wall thickness. Plant, Cell and Environment **34,** 1999–2008.

**Schreiber U, Hormann H, Neubauer C, Klughammer C.** 1995. Assessment of photosystem II photochemical quantum yield by chlorophyll fluorescence quenching analysis. Australian Journal of Plant Physiology **22,** 209–220.

**Siebke K, Ghannoum O, Conroy JP, Badger MR, von Caemmerer S.** 2003. Photosynthetic oxygen exchange in $C_4$ grasses: the role of oxygen as electron acceptor. Plant, Cell and Environment **26,** 1963–1972.

**Silim SN, Ryan N, Kubien DS.** 2010. Temperature response of photosynthesis and respiration in *Populus balsamifera* L.: acclimation versus adaptation. Photosynthesis Research **104,** 19–30.

**Slattery RA, Ort DR.** 2015. Photosynthetic energy conversion efficiency: setting a baseline for gauging future improvements in important food and biofuel crops. Plant Physiology **168,** 383–392.

**Sowinski P, Szczepanik J, Minchin PEH.** 2008. On the mechanism of $C_4$ photosynthetic intermediate exchange between Kranz mesophyll and bundle sheath cells in grasses. Journal of Experimental Botany **59,** 1137–1147.

**Terashima I, Ono K.** 2002. Effects of $HgCl_2$ on $CO_2$ dependence of leaf photosynthesis: evidence indicating involvement of aquaporins in $CO_2$ diffusion across the plasma membrane. Plant and Cell Physiology **43,** 70–78.

**Ubierna N, Sun W, Cousins AB.** 2011. The efficiency of $C_4$ photosynthesis under low light conditions: assumptions and calculations with $CO_2$ isotope discrimination. Journal of Experimental Botany **62,** 3119–3134.

**Ubierna N, Sun W, Kramer DM, Cousins AB.** 2013. The efficiency of $C_4$ photosynthesis under low light conditions in *Zea mays*, *Miscanthus* × *giganteus* and *Flaveria bidentis*. Plant, Cell and Environment **36,** 365–381.

**von Caemmerer S.** 2013. Steady-state models of photosynthesis. Plant, Cell and Environment **36,** 1617–1630.

**von Caemmerer S, Evans JR.** 2015. Temperature responses of mesophyll conductance differ greatly between species. Plant, Cell and Environment **38,** 629–637.

**von Caemmerer S, Furbank RT.** 1999. Modeling $C_4$ photosynthesis. In: Sage RF, Monson RK, eds. $C_4$ plant biology . Toronto: Academic Press, 173–211.

**von Caemmerer S, Ghannoum O, Pengelly JJL, Cousins AB.** 2014. Carbon isotope discrimination as a tool to explore $C_4$ photosynthesis. Journal of Experimental Botany **65,** 3459–3470.

**von Caemmerer S, Quick WP.** 2000. Rubisco: physiology *in vivo*. In: Loogood RC, Sharkey TD, von Caemmerer S, eds. Photosynthesis:

physiology and metabolism . Kluwer Academic Publishers Dordrecht, The Netherlands, 85–113.

**Walker BJ, Ariza LS, Kaines S, Badger MR, Cousins AB.** 2013. Temperature response of *in vivo* Rubisco kinetics and mesophyll conductance in *Arabidopsis thaliana*: comparisons to *Nicotiana tabacum*. Plant, Cell and Environment **36,** 2108–2119.

**Wang Y, Brautigam A, Weber APM, Zhu X-G.** 2014. Three distinct biochemical subtypes of $C_4$ photosynthesis? A modelling analysis. Journal of Experimental Botany **65,** 3567–3578.

**Warren CR, Dreyer E.** 2006. Temperature response of photosynthesis and internal conductance to $CO_2$: results from two independent approaches. Journal of Experimental Botany **57,** 3057–3067.

**Yamori W, Noguchi K, Hanba YT, Terashima I.** 2006. Effects of internal conductance on the temperature dependence of the photosynthetic rate in spinach leaves from contrasting growth temperatures. Plant and Cell Physiology **47,** 1069–1080.

**Yin X, Struik PC.** 2009*a*. $C_3$ and $C_4$ photosynthesis models: an overview from the perspective of crop modelling. NJAS-Wageningen Journal of Life Sciences **57,** 27–38.

**Yin X, Struik PC.** 2009*b*. Theoretical reconsiderations when estimating the mesophyll conductance to $CO_2$ diffusion in leaves of $C_3$ plants by analysis of combined gas exchange and chlorophyll fluorescence measurements. Plant, Cell and Environment **32,** 1513–1524.

**Yin X, Struik PC.** 2012. Mathematical review of the energy transduction stoichiometries of $C_4$ leaf photosynthesis under limiting light. Plant, Cell and Environment **35,** 1299–1312.

**Yin X, Belay DW, van der Putten PEL, Struik PC.** 2014. Accounting for the decrease of photosystem photochemical efficiency with increasing irradiance to estimate quantum yield of leaf photosynthesis. Photosynthesis Research **122,** 323–335.

**Yin X, Struik PC, Romero P, Harbinson J, Evers JB, van der Putten PEL, Vos J.** 2009. Using combined measurements of gas exchange and chlorophyll fluorescence to estimate parameters of a biochemical $C_3$ photosynthesis model: a critical appraisal and a new integrated approach applied to leaves in a wheat (*Triticum aestivum*) canopy. Plant, Cell and Environment **32,** 448–464.

**Yin X, Sun Z, Struik PC, van der Putten PEL, van Ieperen W, Harbinson J.** 2011. Using a biochemical $C_4$-photosynthesis model and combined gas exchange and chlorophyll fluorescence measurements to estimate bundle-sheath conductance of maize leaves differing in age and nitrogen content. Plant, Cell and Environment **34,** 2183–2199.